

Predictive variational inference: Learn the predictively optimal posterior distribution

Jinlin Lai*

Antonio Linero†

Yuling Yao†

March 29, 2026

Abstract

Vanilla variational inference finds an optimal approximation to the Bayesian posterior distribution, but even the exact Bayesian posterior is often not meaningful under model misspecification. We propose predictive variational inference (PVI): a general inference framework that seeks and samples from an optimal posterior density such that the resulting posterior predictive distribution is as close to the true data generating process as possible, while this closeness is measured by multiple scoring rules. By optimizing the objective, the predictive variational inference is generally not the same as, or even attempting to approximate, the Bayesian posterior, even asymptotically. Rather, we interpret it as implicit hierarchical expansion. Further, the learned posterior uncertainty detects heterogeneity of parameters among the population, enabling automatic model diagnosis. This framework applies to both likelihood-exact and likelihood-free models. We demonstrate its application in real data examples.

Keywords: generalized Bayes, variational inference, posterior predictive, simulation-based inference

1. Introduction

Traditional Bayesian inference has often been used for one of two purposes: estimation of parameters θ in a model $p(y|\theta)$ or estimation of a *predictive distribution* $p(\tilde{y}|y)$ to give a probabilistic forecast of a future observation \tilde{y} . In many, such as decision-making, machine learning, or forecasting, the explicit aim is prediction rather than parameter estimation; fortunately, when both the likelihood $p(y|\theta)$ and prior $p^{\text{prior}}(\theta)$ are correctly-specified, traditional Bayesian inference is optimal for both purposes.

There is, however, an increasing awareness of limitations of Bayes under misspecification (Walker, 2013; Gelman et al., 2020; Masegosa, 2020; Huggins and Miller, 2023; Fong et al., 2023). Assume the observations $y = (y_1, \dots, y_n)$ are independent and identically distributed (IID), and denote \tilde{y} to be the next unseen data. The Bayesian posterior predictive distribution of \tilde{y} is the sampling distribution averaged over the posterior density: $p^{\text{Bayes}}(\tilde{y}|y) = \int_{\Theta} p(\tilde{y}|\theta)p(\theta|y)d\theta$. But is this exact Bayesian prediction “optimal”? Or is this Bayesian prediction at least more “optimal” than some point-estimate induced prediction $p(\tilde{y}|\hat{\theta})$ where $\hat{\theta}$ is for example the MLE? The answers are in general both negative (Clarke and Yao, 2024), accompanied by real-data evidence that sometimes Bayesian methods instead produce worse predictions (Wenzel et al., 2020) or overconfident inference (Yang and Zhu, 2018). The only predictive optimality we may assert is that, *if the likelihood and prior are both correct*, then among all probabilistic forecasts, the Bayesian posterior prediction minimizes the posterior-averaged KL divergence from the sampling distribution (Aitchison, 1975), i.e.,

$$\arg \min_{Q(\cdot)} \int \text{KL}(p(\tilde{y}|\theta) || Q(\tilde{y})) p(\theta|y) d\theta = p^{\text{Bayes}}(\tilde{y}|y). \quad (1)$$

*University of Massachusetts Amherst, College of Information and Computer Sciences.

†University of Texas at Austin, Department of Statistics and Data Sciences.

The authors thank Pilar Cossio, Luke Evans, and Erik Thiede for help on cryoEM experiments. This work was partially completed while YY and JL were at the Flatiron Institute.

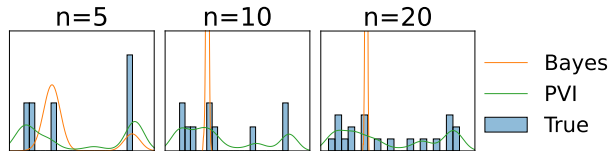


Figure 1: Inference for the molecule angle in a heterogeneous population using cryoEM images. For details, see Section 4.

But this model-being-correct assumption is unlikely relevant to any realistic application. Even if the model is correct, this optimality statement typically does not hold for other divergences practitioners may care about.

To make Bayesian inference under a potential model misspecification, this paper develops *predictive variational inference* (PVI): a general framework that constructs predictively optimal posterior samples $q(\theta|y)$. Unlike classical VI, we optimize a divergence D between the *posterior predictive distribution* and the data generating process $p_{\text{true}}(\tilde{y})$:

$$\min_{q \in \mathcal{F}} D \left(\int_{\Theta} p(\tilde{y}|\theta)q(\theta)d\theta \parallel p_{\text{true}}(\tilde{y}) \right). \quad (2)$$

PVI incorporates various scoring rules, resulting in a family of PVI algorithms each having a statistically meaningful divergence in the objective (2). We typically use a flexible variational family \mathcal{F} such as a normalizing flow (Papamakarios et al., 2021). Rather than viewing this as a sub-optimal approximation to the exact Bayes, PVI directly *learns the optimal predictive distribution* directly. We find three advantages: (a) The PVI-learned optimal predictive is generally different from exact Bayes, even with an infinite amount of data or a flexible enough variational family, while its resulting predictive distribution better fits the observed data. We interpret PVI as an implicit hierarchical expansion. (b) We use PVI as a diagnostic tool. The discrepancy between PVI and exact Bayes is no longer an approximation error; rather, it reveals the *model misspecification*. We use this heuristic to tell which parameter should vary in population to improve the model. (c) PVI applies to both likelihood-exact and likelihood-free settings. Via a simulation-based divergence \mathcal{D} , PVI leads to a computationally efficient tool for simulation-based inference (SBI) tasks. Figure 1 gives a preview of the practical benefits of PVI: We analyze cryogenic electron microscopy (cryoEM) images using a likelihood-free model. The parameter of interest is the bond angle of a molecule, which varies across the population due to molecular heterogeneity. While the exact Bayes posterior quickly collapses to an overconfident point mass, PVI accurately recovers the true population distribution.

1.1. Relationship of PVI to VI

Variational inference (VI, Jordan et al., 1999; Blei et al., 2017) is the workhorse of approximate Bayesian posterior inference for large datasets. Given a sequence observations $y = (y_1, \dots, y_n)$, $y_i \in \Omega$, and parameter vectors $\theta \in \Theta$, instead of sampling from the exact Bayesian posterior density $p(\theta|y)$, VI usually minimizes the Kullback–Leibler (KL) divergence between an approximate inference $q(\theta)$ and the target posterior density $p(\theta|y)$, among a tractable variational family $q \in \mathcal{F}$, $\min_{q \in \mathcal{F}} \text{KL}(q(\theta) \parallel p(\theta|y))$, which is equivalent to maximizing the evidence lower bound (ELBO), the expected log likelihood plus a prior regularization: $\text{ELBO} = \int_{\Theta} \sum_{i=1}^n \log p(y_i|\theta)q(\theta)d\theta - \text{KL}(q(\theta) \parallel p^{\text{prior}}(\theta))$.

VI typically underestimates posterior uncertainty, making VI an inferior approximation to the gold standard Markov chain Monte Carlo (MCMC). On the other hand, the uncertainty reflected in the exact Bayes is not always desirable, as Bayesian inference is conditional on the belief model which is nearly always wrong. In particular, when the sample size n is big enough, the Bernstein–von

Mises theorem ensures that both VI and the exact posterior concentrate to a point mass around the maximum likelihood estimation (MLE). This vanishing posterior uncertainty compromises the flexibility of probabilistic inference: If eventually Bayesian inference is as good as a point estimate even when the model is wrong, then what is the point of investing additional effort into the more challenging task of probabilistic inference?

1.2. Our Contributions and Related Work

Addressing model misspecification has long been an important direction in Bayesian statistics (Berger et al., 1994; Walker, 2013; Gelman and Yao, 2020), and it is beyond the scope of this review to cover all related approaches. When dealing with discrete models, it is well-known that ensemble methods like bagging (Domingos, 1997) and stacking (Le and Clarke, 2017; Yao et al., 2018, 2024) outperform full Bayesian model averaging under misspecification. Conceptually, this present paper shares the same spirit of predictive model averaging and can be viewed as its continuous generalization: instead of a discrete weight on a finite set of models, we find the predicatively-optimal density in a continuous parameter space. Wang et al. (2019); Wang and Blei (2019) build the connection between variational methods and empirical Bayes. Louppe et al. (2019) use adversarial learning to minimize the divergence between the empirical distribution and the marginal distribution of data in SBI settings. Vandegar et al. (2021) approximate the likelihood of those simulators and optimize a neural empirical Bayes prior following the likelihood function. One interesting perspective is that the log score PVI performs neural empirical Bayes by minimizing the prior predictive loss. More related to our method, Masegosa (2020) develops a PAC-Bayes bound and Morningstar et al. (2022) establish PAC^m-Bayes. From a slightly different motivation to minimize the empirical risk gap and ensure the PAC generalization bound, their proposed PAC^m-Bayes solution can be viewed as an instance of our PVI with the special choice of log score, prior regularization, and one version of gradient evaluation. Another line of research focuses on direct loss minimization with expected log predictive density (Sheth and Khardon, 2017, 2020; Jankowiak et al., 2020) for Gaussian processes. Our work provides a practical inference pipeline to directly optimize the log predictive density and many other scoring rules for an arbitrary model.

This work makes four primary contributions. First, we allow for a general scoring rule $S(\cdot, \cdot)$, which allows predictive optimality to be tuned to the scientific task at hand; in addition to the logarithmic score, we provide algorithms that produce calibrated predictive uncertainty (the interval score and CRPS) and the Brier score; the ability to handle divergences other than the logarithmic score is crucial, as CRPS can be implemented in a likelihood-free manner and therefore is amenable to likelihood-free simulation-based inference. Second, we derive gradients estimate for each divergence, including a novel unbiased gradient estimate in the logarithmic score using rejection sampling. Third, we allow for the PVI objective to be regularized either in the direction of the prior distribution or the posterior distribution, allowing us to smoothly interpolate between optimal predictive inference and fully-Bayesian inference. Last, we show how PVI can be used as a diagnostic tool and can motivate model expansion.

2. Predictive variational inference

2.1. Proper scoring rule of predictions

We evaluate probabilistic models by how the resulting posterior prediction fits the observed data. We measure such goodness-of-fit by scoring rules (for a complete review, see e.g., Gneiting and Raftery, 2007). We assume IID observations (y_1, \dots, y_n) on a sample space Ω from an unknown

true data generating process $p_{\text{true}}(y)$, $y \in \Omega$. Let P be a probabilistic forecast for the next unseen data \tilde{y} . A scoring rule is an extended real-valued function $S(P, \tilde{y}) \in \overline{\mathbb{R}}$. The expected score measures the predictive performance of P averaged over the true data generating process $\mathbb{E}[S(P, \tilde{y})] := \int_{\Omega} S(P, \tilde{y}) dp_{\text{true}}(\tilde{y})$, denoted by $S(P, p_{\text{true}})$, and is often approximated by the empirical score $S(P, p_{\text{true}}) \approx \frac{1}{n} \sum_{i=1}^n S(P, y_i)$. A scoring rule is said to be proper if the maximum expected score is achieved under the truth, i.e., $S(P, p_{\text{true}}) \leq S(p_{\text{true}}, p_{\text{true}})$. A proper scoring rule corresponds to a divergence function in the Ω space between the forecast P and the true data generating process p_{true} , $D(P, p_{\text{true}}) = S(p_{\text{true}}, p_{\text{true}}) - S(P, p_{\text{true}})$. The most common score is the log score, $S(P, \tilde{y}) = \log P(\tilde{y})$, which leads to the familiar KL divergence. Different scoring rules evaluate different aspects of the prediction, such as the predictive density, quantiles and coverage.

2.2. Optimizing the predictive performance

Consider the following inference task: We observe data $y = (y_1, \dots, y_n)$, $y_i \in \Omega$, and assume $\{y_i\}$ are conditionally IID given covariates. Omitting covariates for brevity, we denote $p_{\text{true}}(y_i)$ as the data generating process. We are given a (potentially wrong) model with a parameter vector $\theta \in \Theta$, a (potentially intractable) likelihood $p(y_i|\theta)$, and a prior $p^{\text{prior}}(\theta)$. Let $p(\theta|y) \propto p^{\text{prior}}(\theta) \prod_{i=1}^n p(y_i|\theta)$ be the exact Bayesian posterior density. Our inferential goal is a variational approximation $q_{\phi}(\theta)$, parameterized by a variational parameter $\phi \in \Phi$. Averaged over the inference q_{ϕ} , the posterior predictive distribution of the next unseen data \tilde{y} will be $q_{\phi}^Y(\tilde{y}) := \int q_{\phi}(\theta) p(\tilde{y}|\theta) d\theta$. So far the setting is the same as standard VI. However, rather than approximating exact Bayes, we first pick a proper scoring rule S on the outcome predictions, and then optimize ϕ such that the empirical scoring rule of the posterior predictive distribution is maximized. That is,

$$\max_{\phi \in \Phi} \left(\sum_{i=1}^n S \left(\int_{\Theta} p(\cdot|\theta) q_{\phi}(\theta) d\theta, y_i \right) - \lambda r(\phi) \right), \quad (3)$$

where $r(\phi)$ is an optional regularizer. If we choose S to be the log score, PVI maximizes the usual log predictive density $\max_{\phi \in \Phi} \sum_{i=1}^n \log \int_{\Theta} p(y_i|\theta) q_{\phi}(\theta) d\theta$. Equivalently, as in (2), we can describe PVI as minimizing the divergence between the posterior predictive distribution, $q_{\phi}^Y(\tilde{y})$, and the true data generating process of the next unseen observation $p_{\text{true}}(\tilde{y})$. Let D be the corresponding divergence of the scoring rule S . Then up to a constant C , the entropy of $p_{\text{true}}(\tilde{y})$, the first summation in the PVI objective (3) is the negative empirical version of this outcome-space divergence: $\lim_{n \rightarrow \infty} \sum_{i=1}^n S(q_{\phi}^Y(\cdot), y_i) / n - C = -D(q_{\phi}^Y(\tilde{y}) \parallel p_{\text{true}}(\tilde{y}))$. For example, the log score PVI minimizes the KL divergence to $p_{\text{true}}(\tilde{y})$.

2.3. Regularization

We include a tunable regularization term $-\lambda r(\phi)$ in the PVI objective (3). There are two reasons for this. First, compared to a empirical risk minimization, it is a salient feature of Bayes to incorporate prior knowledge, which we will keep. Second, regularization makes the improves the identifiability of ϕ . The optima is not necessarily unique in the PVI optimization of (3), and adding a regularizer stabilizes the location of the final solution. We consider two regularizers: regularizing to the prior, or to the posterior.

$$r^{\text{prior}}(\phi) = \text{KL}(q_{\phi}(\theta) \parallel p^{\text{prior}}(\theta)). \quad (4)$$

$$r^{\text{post}}(\phi) = \text{KL}(q_{\phi}(\theta) \parallel p(\theta|y)). \quad (5)$$

Regularization toward the prior (4) is familiar, as it has appears in both standard VI and other generalized VI methods (see Section 5). The posterior-orientated regularization (5) is unique to PVI, and it is effectively the ELBO in standard VI. With this term, PVI can continuously interpolate between the pure prediction-optimization ($\lambda = 0$) and pure Bayes ($\lambda = \infty$), and thereby benefit from both finite-sample robustness and large-sample optimality guarantees. In most experiments, we keep λ as a small fixed constant, though in principle it can also be tuned using cross-validation. See Supplement B.1 for more demonstrations of the effect of the regularization.

2.4. Asymptotics and hierarchical Bayes

Before we demonstrate the practical implementation of PVI (3) and various choices of S , we prove some appealing theoretical properties of the PVI optima. With enough samples and under certain assumptions, one would expect that the posterior prediction of the PVI solution converges to the best possible probabilistic forecast:

Proposition 1 (informal). *Let the variational distribution $q_\phi(\theta)$ be parameterized by $\phi \in \Phi$. With any strictly proper score function S , an unknown true data generating process distribution $p_{\text{true}}(y)$, a likelihood model $p(y|\theta)$, and a size- n sample $y_1, y_2, \dots, y_n \sim p_{\text{true}}(\cdot)$, let ϕ_n be the solution of the PVI objective (3) with a continuous prior regularization on ϕ . The predictive optimal variational parameter ϕ_0 is defined as*

$$\phi_0 := \operatorname{argmax}_{\phi \in \Phi} S \left(\int_{\Theta} p(\cdot|\theta) q_\phi(\theta) d\theta, p_{\text{true}}(\cdot) \right).$$

Define $\ell(y, \phi) = S(\int p(\cdot|\theta) q_\phi(\theta) d\theta, y)$, then under regularity conditions, we have (1) consistency: $\phi_n \xrightarrow{P} \phi_0$ as $n \rightarrow \infty$; (2) asymptotic normality: $\sqrt{n}(\phi_n - \phi_0) \xrightarrow{d} \mathcal{N}(0, V)$ where V is a non-singular matrix.

The detailed proposition and proof is available in Supplement A.1. This consistency entails two corollaries.

Corollary 1. *If the model is well-specified, i.e., there exists a θ_0 and ϕ^* such that $p(y|\theta_0) = p_{\text{true}}(y)$ and $q_{\phi^*}(\theta) = \delta_{\theta_0}(\theta)$, then under regularity conditions, $\phi_n \xrightarrow{P} \phi^*$.*

Corollary 2. *If the model is misspecified but there exists a ϕ^* such that $p_{\text{true}}(y) = \int p(y|\theta) q_{\phi^*}(\theta) d\theta$, then under regularity conditions, $\phi_n \xrightarrow{P} \phi^*$.*

The corollaries establish the backward compatibility of PVI when the variational family is flexible: If the model is well-specified, PVI concentrates on the true parameter, the same as regular Bayesian methods. However, if the model contains a parameter that varies in population, while the regular Bayes still concentrates, PVI asymptotically converges to the true population distribution of the parameter, not a point mass. We use a toy example to illustrate this difference.

A normal example. We model an IID dataset $\{y_i\}_{i=1}^n$ by a model $y|\theta \sim \text{normal}(\theta, 1)$ where the only parameter is the location θ . The unknown true data generating procedure is $y_i \sim \text{normal}(0, \sigma_{\text{true}})$. The exact posterior is $p(\theta|y) = \text{normal}(\theta | \bar{y}, 1/\sqrt{n})$. We use PVI with a Gaussian variational family. (a) When $\sigma_{\text{true}} = 1$, the model is well-specified, and PVI solution $q(\theta)$ converges to the point mass at 0, same as the classical VI and Bayes. (b) When $\sigma_{\text{true}} = 2$, while the regular Bayes still concentrates to the point mass at 0, the PVI posterior converges to $\text{normal}(0, \sqrt{3})$, and stays there as n goes to infinity regardless of the scoring rule, so that the posterior prediction matches the

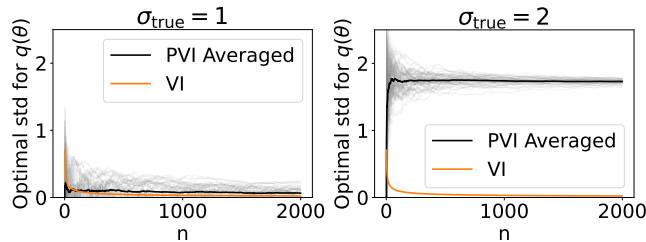


Figure 2: Optimal standard deviation of $q(\theta)$ with PVI or VI for the simple normal case from 50 simulations, with $\sigma_{true} = 1$ on the left and $\sigma_{true} = 2$ on the right.

true data process despite the model being wrong. In general, unlike standard Bayesian inference, when the model is misspecified the PVI posterior uncertainty may not go to zero as the sample size grows to infinity, a reflection of the “epistemic humility”. See Fig. 2 for simulations.

2.5. Heterogeneity detection and implicit hierarchical Bayes

As implied by Corollary 1, a non-vanishing PVI posterior variance indicates model misspecification, which we can use as a diagnostic check¹. In addition to a binary correct-or-wrong model check, monitoring the PVI posterior variance further indicates whether the parameters need to vary in population. With large enough n , if the variance of a variable $\text{Var}(\theta_i) > \alpha$, where α is a chosen threshold, we may need to expand the model. We call this check “heterogeneity detection”. We demonstrate how to use PVI to guide model expansion using an election example in Section 4.2. Another possible indicator of heterogeneity is the difference between the forecast scores with PVI and VI posteriors.

The parameter-may-vary-in-the-population perspective is the key motivation behind Bayesian hierarchical modeling (Gelman, 2006). Given any IID observational model $y \sim p(y|\theta)$, we distinguish between three views of inference:

1. *Complete-pooling* view: We perform standard Bayesian inference $\theta|y$. It is straightforward but more prone to model misspecification.
2. *Full-hierarchical* view: Any parameter is assumed to vary in the population and we aim for a fully individualized inference. That is, we expand the model as $y_i \sim p(y|\theta_i)$, and infer $\theta|y$ where $\theta = (\theta_1, \dots, \theta_n)$. This hierarchical expansion makes the model more robust (Wang and Blei, 2018), with the cost of augmenting each parameter θ by n copies $\theta_1, \dots, \theta_n$, which quickly becomes computationally prohibitive when n is big. Moreover, as each parameter θ_i only links to one data point y_i , this individualized inference is typically noisy and relies on the hyper-prior, which itself is a parametric family and may be misspecified.
3. *Implicit-hierarchical* view: We implicitly adopt the view of $y_i \sim p(y_i|\theta_i)$, but we marginalize out individual θ_i and only infer their population distribution $\theta_1, \theta_2, \dots, \theta_n \sim \pi_{\text{pop}}(\theta)$. In many cases, the primary inference interest lies in this population distribution, such as understanding population-level properties or making predictions for new data points.

PVI is an implicit hierarchical expansion. Under the condition of Corollary 2, $q_\phi(\theta)$ converges to $\pi_{\text{pop}}(\theta)$, the above-mentioned population distribution of parameters, offering an automated and computationally-fast way to perform hierarchical expansion for any model, and adapting to any scoring rules.

¹As a caveat, the regularity condition in Corollary 1 contains a uniqueness assumption which may not always hold.

Rule	Objective to maximize	Gradient estimator
Logarithmic score	$\sum_{i=1}^n \log \int_{\Theta} p(y_i \theta)q_{\phi}(\theta)d\theta$	$\boxed{a} \left \sum_{i=1}^n \left(\sum_{j=1}^M \frac{d}{d\phi} p(y_i T_{\phi}(u_j)) \right) / \left(\sum_{j=1}^M p(y_i T_{\phi}(u_j)) \right) \right $ $\boxed{b} \left \sum_{i=1}^n \frac{\sum_{j=1}^M (\mathbb{1}(t_j < p(y_i \theta_j)/C) \frac{\partial}{\partial \phi} \log q_{\phi}(\theta_j))}{\sum_{j=1}^M \mathbb{1}(t_j < p(y_i \theta_j)/C)} \right $
Quadratic score	$\sum_{i=1}^n 2 \int_{\Theta} f(\theta, y_i)q_{\phi}(\theta)d\theta$ $-\sum_{j=1}^I \left(\int_{\Theta} f(\theta, j)q_{\phi}(\theta)d\theta \right)^2$	$2 \sum_{i=1}^n \frac{1}{M} \sum_{j=1}^M f(T_{\phi}(u_j), y_i)$ $-\sum_{j=1}^I \left(\frac{1}{M} \sum_{k=1}^M f(T_{\phi}(u_k), j) \right) \left(\frac{1}{M} \sum_{k=1}^M \frac{df(T_{\phi}(u_k), j)}{d\phi} \right)$
Interval score	$-\sum_{i=1}^n (U_{\alpha} - L_{\alpha}) + \frac{2}{\alpha} (L_{\alpha} - y_i) \mathbb{I}(y_i < L_{\alpha})$ $+\frac{2}{\alpha} (y_i - U_{\alpha}) \mathbb{I}(y_i > U_{\alpha})$	$\sum_{i=1}^n \frac{\partial \hat{U}_{\alpha}}{\partial \phi} \left(\frac{2}{\alpha} \mathbb{I}(y_i > \hat{U}_{\alpha}) - 1 \right) - \frac{\partial \hat{L}_{\alpha}}{\partial \phi} \left(\frac{2}{\alpha} \mathbb{I}(y_i < \hat{L}_{\alpha}) - 1 \right)$
CRPS	$-\sum_{i=1}^n \mathbb{E}_{y^{\text{sim}} \sim \int_{\Theta} p(y \theta)q_{\phi}(\theta)d\theta} [y^{\text{sim}} - y_i]$ $+\frac{1}{2} \mathbb{E}_{y_1^{\text{sim}}, y_2^{\text{sim}} \sim \int_{\Theta} p(y \theta)q_{\phi}(\theta)d\theta} [y_1^{\text{sim}} - y_2^{\text{sim}}]$	$-\frac{1}{2M} \sum_{i=1}^n \sum_{m=1}^{2M} (g_m \cdot \text{sign}(y_m^{\text{sim}} - y_i))$ $+\frac{1}{2M} \sum_{m=1}^M ((g_m - g_{m+M}) \cdot \text{sign}(y_m^{\text{sim}} + y_{m+M}^{\text{sim}}))$

Table 1: How to compute the objectives and their gradients for four scoring rules. Here, $\theta = T_{\phi}(u), u \sim q(\cdot)$ is a reparameterization such that $\theta \sim q_{\phi}(\cdot)$. We generate $2M$ independent observations $y_1^{\text{sim}}, \dots, y_{2M}^{\text{sim}}$ for CRPS and denote $g_m = \frac{d}{d\phi} y_m^{\text{sim}}$ for $m = 1, \dots, 2M$. We estimate sample quantiles \hat{L}_{α} and \hat{U}_{α} for the interval score from simulated observations.

3. Implementation and gradient evaluation

PVI is a natural idea, but its optimization is nontrivial. This section provides practical stochastic gradient algorithms to implement PVI (3) on four concrete scoring rules S : the logarithmic, quadratic, interval and continuous ranked probability score.

The PVI objective (3) contains two terms. The regularization term is the usual ELBO (posterior regularizer) or part of the ELBO (prior regularizer), hence its gradient with respect to the variational parameter ϕ is straightforward. The first term in (3) is a summation: $R(\phi) := \sum_{i=1}^n S(\int p(\cdot|\theta)q_{\phi}(\theta)d\theta, y_i)$. In stochastic optimization, in each iteration we sample a mini-batch of $\theta_1, \dots, \theta_M$ draws from the variational density $q_{\phi}(\theta)$. To iteratively update ϕ , we need to evaluate the gradient $\frac{d}{d\phi} R(\phi)$. As an overview, we summarize the evaluation of $R(\phi)$ and the gradient $\frac{d}{d\phi} R(\phi)$ in Table 1. We defer theoretical claims and algorithm details to the Supplement A.

The logarithmic score with unbiased gradient $S(Q, y) = \log Q(y)$ is the default score in Bayesian inference. The log-score PVI equipped with the prior regularization and the asymptotically unbiased gradient (a) coincides with the PAC^m-Bayes (Morningstar et al., 2022). Because of the exchange in the order of the integral and log, the objective $R(\phi)$ contains the logarithm of a stochastic summation, making its gradient evaluation nontrivial. Table 1 shows two gradient estimates $\frac{d}{d\phi} R(\phi)$. The first estimate approximates the integral by reparameterization, and we show it is asymptotically unbiased when the batch size M is big. With finite batch size, however, the gradient estimator is biased. In the extreme case of $M = 1$, the bias is so severe that the gradient reduces to that of standard VI. To correct for for this finite-batch bias, we further develop a second novel gradient estimate based on rejection-sampling. For this gradient, at each SGD iteration given a ϕ , we draw M IID copies $\theta_1, \dots, \theta_M$ from $q_{\phi}(\theta)$, and M i.i.d. copies t_1, \dots, t_M from Uniform(0,1) distribution. For each j , we compute $p(y_i|\theta_j)/C$. If $t_j < p(y_i|\theta_j)/C$ then we accept the draw θ_j for

y_i . If at least one draw is accepted we approximate $g_i^{\log}(\phi) = \frac{d}{d\phi} \log \int p(y_i|\theta)q_\phi(\theta)d\theta$ by

$$g_i^{\text{RS}} := \frac{\sum_{j=1}^M \left(\mathbb{1}(t_j < p(y_i|\theta_j)/C) \frac{\partial}{\partial \phi} \log q_\phi(\theta_j) \right)}{\sum_{j=1}^M \mathbb{1}(t_j < p(y_i|\theta_j)/C)}. \quad (6)$$

We show that this novel gradient estimate (6) is always unbiased, regardless of the batch size, and hence guaranties the SGD convergence under regular conditions.

Proposition 2. *For any $M \geq 1$, $\mathbb{E}_{\theta,t}[g_i^{\text{RS}}] = g_i^{\log}(\phi)$.*

See Supplement A.2 for proofs and more details.

The quadratic score or equivalently the Brier score (Brier, 1950) is useful to examine predictions on categorical-valued outcomes, $y_i \in \Omega = \{1, 2, \dots, I\}$. It is sometimes more sensitive than the log score for prediction evaluations (Selten, 1998). To run PVI, we count the occurrences in the data: category i has n_i occurrences. Denote the conditional predictive mass function, $f(\theta, y_i) = \Pr(Y = y_i|\Theta = \theta)$, the posterior predictive distribution is $\Pr(Y = y_i) = \int_{\Theta} f(\theta, y_i)q_\phi(\theta)d\theta$. We present the objective and its gradient estimator in the second row of Table 1. In the supplement, we show that this gradient evaluation converges in probability and leads to a valid PVI optimization.

The interval score (IS, Dunsmore, 1968; Winkler and Murphy, 1968) measures the sharpness and calibration of the predictive intervals given true data. Suppose $y \in \mathbb{R}$. Under the significance level α , the probabilistic forecast Q corresponds to the prediction interval $[L_\alpha, U_\alpha]$. The objective of interval score is in the third row of Table 1. In PVI, we need to optimize the parameter ϕ by minimizing the interval score of the predictive model $Q_\phi(y) = \int_{\Theta} p(y|\theta)q_\phi(\theta)d\theta$. However, it may be hard to derive L_α and U_α analytically. Instead, we generate M samples, estimate the sample quantiles \hat{L}_α and \hat{U}_α , and compute the IS using the quantile estimates. During optimization, we use the gradients of estimated quantiles from autodiff, $\frac{\partial \hat{L}_\alpha}{\partial \phi}$ and $\frac{\partial \hat{U}_\alpha}{\partial \phi}$. In the supplement, we show these gradient estimators are convergent.

The continuous ranked probability score (CRPS, Matheson and Winkler, 1976) measures the L^2 distance between the cumulative density functions (CDF) of the prediction and true data generating distribution. It could be interpreted as the combination of IS across all significance levels (Gneiting and Ranjan, 2011). To start, assume the observation $y_i \in \mathbb{R}$ is a scalar. Typically neither the true nor the predicted CDF is of a closed-form, and we evaluate the CRPS via the simulations from the posterior predictions: all we need is to draw θ from $q_\phi(\theta)$, and then y^{sim} from $p(y|\theta)$ in sequence. The fourth row of Table 1 presents the CRPS objectives, and its gradient. Our estimates only require simulations y^{sim} from the posterior predictive, not the density, making it readily usable for simulation-based inference (SBI). We prove this gradient is always unbiased as long as y^{sim} can be differentiated through, leading to a stronger convergence guarantee for the optimization.

Although the original CRPS is designed for one-dimensional outcomes, it naturally extends to higher dimensional outcomes by replacing the scalar absolute value $|\cdot|$ in the objective with a non-negative, continuous negative-definite kernel function (for details, see Gneiting and Raftery, 2007). In our experiment when the outcome y_i is high-dimensional microscopy images, we simply plug in the L^2 distance between observed y_i and simulations y^{sim} in the CRPS and gradient evaluation, which is still a valid proper scoring rule.

PVI in likelihood-free inference. Many recent scientific applications involve intractable likelihood: the sampling distribution $p(y|\theta)$ may contain a complex simulator, such that we cannot evaluate

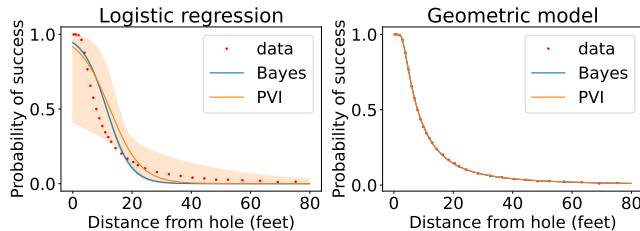


Figure 3: Posterior predictive distribution of two different models of the golf putting problem, with either Bayesian posterior or PVI posterior.

the conditional density $p(y|\theta)$ but still can draw simulations y^{sim} from it. Simulation-based inference (SBI, Cranmer et al., 2020) is a successful tool for likelihood-free tasks, but the best an SBI algorithm can achieve is to be faithful to the Bayesian posterior, which may suffer from model-misspecification (e.g., Cannon et al., 2022). In contrast, because we have developed the general PVI method incorporating an arbitrary scoring rule, we handle likelihood-exact and -free inference in a unified framework. In particular, our proposed PVI with CRPS is well-suited for such likelihood-free applications: All we need is a continuous outcome space ($y \sim \mathbb{R}^d$) and a differentiable simulator. For all the reasoning before, PVI is more robust against model misspecification and better fits the true data process. In our later cryoEM experiment in Sec. 4.3, we use PVI-CRPS to learn the population distribution of frozen molecules with a simulator. Here, the PVI-learned $q_\phi(\cdot)$ is not merely a prediction-oriented augmentation, but a physically meaningful quantity.

4. Experiments

We present three examples. We show how PVI is used as a tool for detecting model mis-specification in a golf putting model. In the election example, we use PVI as a heterogeneity detection and a diagnosis for model expansion. In a cryoEM example, we apply PVI to infer protein structures from intractable likelihood. Additional experiments and benchmarks are in Supplement B.

4.1. Model misspecification detection for golf putting

Gelman and Nolan (2002) modeled the proportion of successful putts from professional golfers as a function of distance from the hole. There are two models for the problem: the logistic regression model and the geometric model. We plot the posterior predictive distribution of both models with either the Bayesian or PVI posterior in Figure 3. Note that logistic regression is misspecified so the Bayesian posterior struggles to fit the curve and selects a narrow and incorrect prediction. But such misspecification is addressed by PVI with a wider posterior. The geometric model fits the data well, and both the Bayesian and PVI posterior select the correct parameters. This indicates that PVI can be used as a tool for misspecification detection. When a wide posterior is observed, we should modify the model for better fit. We will demonstrate further with the election model next.

4.2. Model expansion in U.S. election analysis

We now apply PVI to analyze US presidential election that was previously studied by Ghitza and Gelman (2013). We use the Current Population Survey’s (CPS) post-election voting and registration supplement in the Year 2000 ($N = 68,643$ respondents) to fit a binomial regression model that predicts the voting turnouts given a respondent’s state ($\{1, 2, \dots, 51\}$ including D.C.), ethnicity group ($\{1, 2, 3, 4\}$) and income level ($\{1, 2, \dots, 5\}$). Bayesian multilevel modeling typically starts by modeling the marginal state-, ethnicity- and income-effects. Next, the income effect may vary by

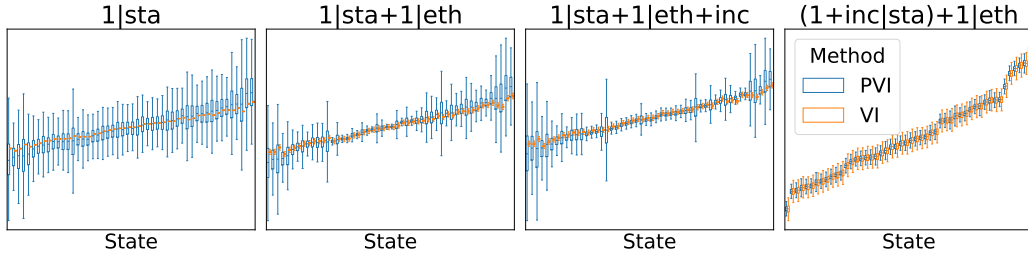


Figure 4: Distribution of inferred logit across states with $x = 1$ for ethnic group 1 from four different voting models. To focus on the variability across states, we set $\beta_{2,1}$ to its sample mean.

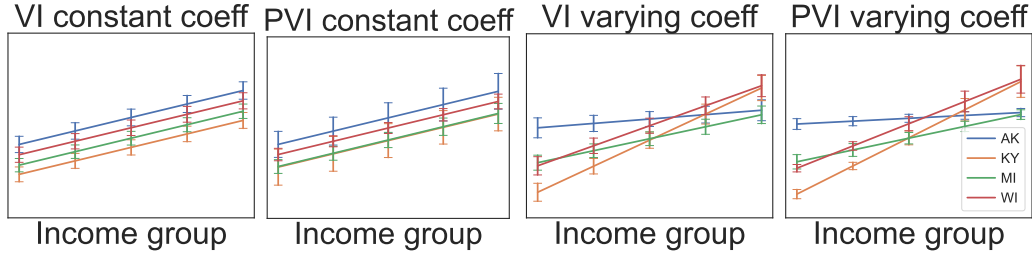


Figure 5: Regression logits of four states learned from the Current Population Survey’s (CPS) post-election voting and registration supplement in 2000. Unrelated parameters are replaced by their sample means. Two models are compared: one with a constant coefficient, and one with varying coefficients among states.

state, so it makes sense to model the two-way interactions, and then the three-way interactions. Hence, even in a simple binomial regression with full interactions, we have at least $51 \times 5 \times 4 = 1,020$ coefficient parameters. But it is still not saturated: there are still many unobserved confounders and hence this state \times income \times ethnicity effect may vary in the population, and an individualized fully-hierarchical model expansion (Sec.2.4) would contain $1,020 \times 68,643 = 70$ million parameters. We need some guidance on how deep the interactions we want to include in the model.

To test how PVI helps model check and further guides iterative model building, we first generate synthetic data so that we can compare the inference with a ground truth. In the survey data, in the n -th cell defined by the state i_n , ethnicity group j_n , and income level x_n , out of N_n total respondents, y_n of them are positive outcomes ($1 =$ turnout). We simulate a dataset from a generating process:

$$y_n \sim \text{Binomial}(N_n, \text{Logit}^{-1}(\beta_{1,i_n} + \beta_{2,j_n} + \beta_{3,i_n}x_n)),$$

where $\beta_1 \in \mathbb{R}^{51}$, $\beta_2 \in \mathbb{R}^4$, $\beta_3 \in \mathbb{R}^{51}$. Now we run inference (our PVI and classical VI) on the well-specified model and three incomplete/misspecified models

$$\begin{aligned} y_n &\sim \text{Binomial}(N_n, \text{Logit}^{-1}(\beta_{1,i_n})), \\ y_n &\sim \text{Binomial}(N_n, \text{Logit}^{-1}(\beta_{1,i_n} + \beta_{2,j_n})), \\ y_n &\sim \text{Binomial}(N_n, \text{Logit}^{-1}(\beta_{1,i_n} + \beta_{2,j_n} + \beta_3 x_n)). \end{aligned}$$

Figure 4 demonstrates the inferred logits across states with different models. Despite models being misspecified, VI always concentrates, while our PVI correctly picks a wider variational distribution, evidence we regard as evidence of model misspecification. This illustrates PVI’s value for model checking; the closer a statistical model is to the true model, the less posterior PVI variability is observed. In the last subfigure, PVI posterior successfully concentrates when the model is correctly specified, converging to the same parameters as VI.

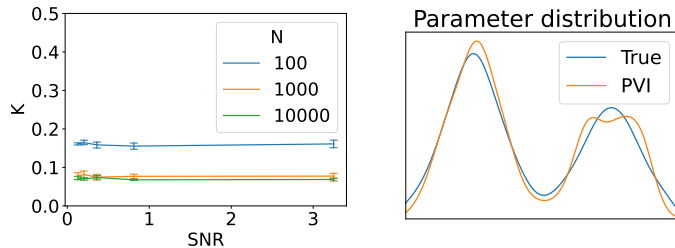


Figure 6: Parameter inference for cryoEM with PVI. In the first panel, the y-axis reports the gap K between the inferred distribution and the true distribution with varying SNR and sample size, where the K is computed from a two-sample KS test. The second figure demonstrates that PVI inferred posterior distribution accurately recovers the true distribution in a realistic setting when $N = 10,000$ and $\text{SNR} \approx 0.13$.

Next, in the real data analysis, we fit two models both using PVI and VI: a model with (a) a constant coefficient across states, and (b) varying coefficients across states. We plot the logits of four different states in Figure 5 to demonstrate the behaviors of PVI. PVI on the constant coefficient model reveals that the posterior variances of some states (AK, KY) are higher than other states, suggesting that we should expand the model to allow varying coefficients in these states, which agrees with the conclusion of Ghitza and Gelman (2013). In the varying coefficients model, the two states indeed have different slopes. In contrast, VI assigns equal variances to all parameters, regardless of whether the model is wrong.

4.3. Likelihood-free cryoEM inference

Inferring the structures of proteins is a challenging problem for computational biology. With the technique of cryo-electron microscopy (cryoEM, Nogales, 2016; Singer and Sigworth, 2020), scientists obtain a large collection of 2D protein images.

Recently, Dingeldein et al. (2024) used SBI to analyze cryoEM images. The parameter of interest θ represents the protein structure, the sampling model of images follows $\mathbf{y} = f(\theta, \epsilon)$, where $\epsilon \sim p^{\text{noise}}(\cdot)$ represents other nuisance parameters (rotations, translations, and measurement errors). The simulator is differentiable, but the likelihood $p(\mathbf{y}|\theta)$ is intractable because it is difficult to integrate all parameters. Moreover, the protein structure θ is not one single fixed truth across all images: the proteins were distributed via their free energy distribution when they were frozen. Due to computational challenges, this protein dynamic is not fully addressed in past works, which only attempt to approximate the exact but overconfident Bayes posterior $\theta|\mathbf{y}$ even when the image sample size N is big. We use CRPS-equipped PVI to find an optimal ϕ , such that the simulations from $\int_{\Theta} p(y|\theta)q_{\phi}(\theta)d\theta$ match the observed images as close as possible under the CRPS metric. This approach is computationally efficient as it does not need likelihood evaluations or expensive prior simulations. The learning of the θ -distribution is effectively nonparametric as we use a normalizing flow.

We work with a realistic simulator of heat shock proteins (HSP90, Whitesell and Lindquist, 2005). An HSP90 protein contains two chains where the opening θ controls the conformation. We choose a parameter distribution with two modes and generate a synthetic dataset of noisy images. In the simulator, the noise includes a normal error and a random defocus for the contrast transfer function (CTF) of lens, making the signal-to-noise ratio (SNR) of images very low. Figure 1 shows that the variational posterior $q_{\phi}(\cdot)$ learned from PVI with CRPS quickly matches the population ground-truth openings of the protein population, while the Bayes posterior ignores heterogeneity and collapses to point estimates. Figure 6 visualizes the accuracy of PVI posterior as a function of

SNR and sample size: the PVI posterior converges to the target even with a low SNR.

5. Discussion

Generalized VI and generalized Bayes. It is not a new idea to reframe Bayesian inference as an infinite dimensional optimization. As mathematically equivalent to (1), Zellner (1988) stated that the minimizer of $\mathbb{E}_{\theta \sim q(\cdot)} \sum_{i=1}^n [-\log p(y_i|\theta)] + \text{KL}(q \parallel p^{\text{prior}})$ is the classical Bayesian posterior $q(\cdot) = p(\cdot|y)$, while the vanilla VI is the solution of the constrained optimization. Motivated by this view, many variations of Bayes have emerged. Knoblauch et al. (2022) define a “generalized VI” framework (rule-of-three), $\min_{q \in \mathcal{F}} \mathbb{E}_{\theta \sim q(\cdot)} (\sum_{i=1}^n l(y_i, \theta)) + D(q \parallel p^{\text{prior}})$, where the user can choose a $(y \times \theta)$ -space loss function $l(y_i, \theta)$, a θ -space divergence D , and a feasible region \mathcal{F} , and this framework includes many other generalized-VIs as special cases such as decision-theory-based-VI (Lacoste-Julien et al., 2011; Kuśmierczyk et al., 2019), and Gibbs-VI (Alquier et al., 2016). In the same vein, Bissiri et al. (2016) study a generalized Bayes framework: given a $(y \times \theta)$ -space loss function $l(y_i, \theta)$, an unnormalized posterior is defined by $\exp[-\sum_{i=1}^n l(\theta, y_i)] p^{\text{prior}}(\theta)$, a generalization of the PAC- and Gibbs-posterior (Zhang, 2006; Jiang and Tanner, 2008). Grünwald and Van Ommen (2017) introduce a learning rate η to the Bayes model, which controls how close the posterior should be to the prior. When the likelihood is intractable, Matsubara et al. (2022) use Stein discrepancy as a loss function in generalized Bayes.

Our posterior-predictive-centric PVI framework is spiritually different from existing generalized-Bayes and -VI procedures. To see their difference, take the default loss function, the negative log likelihood, $l(y, \theta) = -\log p(y|\theta)$, and D to be the KL divergence, then both generalized VI and generalized Bayes degenerate to the vanilla Bayes posterior. In contrast, the PVI posterior under the default logarithm score is generally not the same, even asymptotically, as the vanilla Bayes posterior. Even with the same log score, PVI and the generalized VI differ in the position of log and the integral — PVI evaluates the global predictive performance of the posterior-averaged predictive distribution, while the generalized VI assesses the posterior-averaged local predictive performance.

Limitations and future directions. In this paper, we made minimal tuning on PVI for a fair comparison. There is large room for fine-tuning (tuning λ , interpolating between the prior and posterior regularization, choice of scoring rules and combinations, variance reduction of the stochastic gradient, etc.), which we defer for future engineering. Throughout the paper, we have relied on the assumption that observations are conditionally IID given covariates, or at least exchangeable, which is a limitation compared with the regular Bayes. This IID requirement is shared by any scoring-rule-based model evaluation, generalized VI, and any loss-function-based learning algorithm. We can extend our current IID PVI to complex data structures; it requires defining internal replications and is beyond this paper.

Theoretically we justify PVI via asymptotic optimality. It is useful to further study its finite sample rate, and compare the convergence rate under various scoring rules. Another direction is to use finite-sample conformality as the objective. Unlike regular Bayes which may be overconfident, the parameter uncertainty in PVI can grow as a function of sample size (Fig. 2), and may not shrink to zero. In a concurrent work, McLatchie et al. (2025) show that under the correct model, predictive oriented posteriors may shrink to the true parameter in a slower convergence rate than the regular Bayesian posterior. Such differences can also be observed in Figure 2. This implies the heterogeneity detection with posterior variance may be flawed: although the heterogeneity can be detected in the limit, with finite samples, it is unclear whether the variance comes from model mis-specification or the slow convergence rate. Nevertheless, PVI can still be used as a tool to augment the predictive

performance of Bayesian models.

References

- Aitchison, J. (1975). Goodness of prediction fit. *Biometrika*, 62(3):547–554.
- Alquier, P., Ridgway, J., and Chopin, N. (2016). On the properties of variational approximations of Gibbs posteriors. *Journal of Machine Learning Research*, 17(236):1–41.
- Berger, J. O., Moreno, E., Pericchi, L. R., Bayarri, M. J., Bernardo, J. M., Cano, J. A., De la Horra, J., Martín, J., Ríos-Insúa, D., and Betrò, B. (1994). An overview of robust Bayesian analysis. *Test*, 3(1):5–124.
- Bissiri, P. G., Holmes, C. C., and Walker, S. G. (2016). A general framework for updating belief distributions. *Journal of the Royal Statistical Society: Series B*, 78(5):1103–1130.
- Blei, D. M., Kucukelbir, A., and McAuliffe, J. D. (2017). Variational inference: A review for statisticians. *Journal of the American statistical Association*, 112(518):859–877.
- Brier, G. W. (1950). Verification of forecasts expressed in terms of probability. *Monthly Weather Review*, 78(1):1–3.
- Cannon, P., Ward, D., and Schmon, S. M. (2022). Investigating the impact of model misspecification in neural simulation-based inference. *arXiv:2209.01845*.
- Clarke, B. and Yao, Y. (2024). A cheat sheet for Bayesian prediction. *arXiv:2304.12218*.
- Cranmer, K., Brehmer, J., and Louppe, G. (2020). The frontier of simulation-based inference. *Proceedings of the National Academy of Sciences*, 117(48):30055–30062.
- Dingeldein, L., Silva-Sánchez, D., Evans, L., D’Imprima, E., Grigorieff, N., Covino, R., and Cossio, P. (2024). Amortized template-matching of molecular conformations from cryo-electron microscopy images using simulation-based inference. *bioRxiv*, pages 2024–07.
- Domingos, P. M. (1997). Why does bagging work? a Bayesian account and its implications. In *KDD*, pages 155–158.
- Dunsmore, I. (1968). A bayesian approach to calibration. *Journal of the Royal Statistical Society: Series B (Methodological)*, 30(2):396–405.
- Durkan, C., Bekasov, A., Murray, I., and Papamakarios, G. (2019). Neural spline flows. *Advances in Neural Information Processing Systems*, 32.
- Fong, E., Holmes, C., and Walker, S. G. (2023). Martingale posterior distributions. *Journal of the Royal Statistical Society Series B*, 85(5):1357–1391.
- Gelman, A. (2006). Multilevel (hierarchical) modeling: What it can and cannot do. *Technometrics*, 48(3):432–435.
- Gelman, A. (2007). *Data analysis using regression and multilevel/hierarchical models*. Cambridge university press.
- Gelman, A. and Nolan, D. (2002). A probability model for golf putting. *Teaching statistics*, 24(3):93–95.
- Gelman, A., Vehtari, A., Simpson, D., Margossian, C. C., Carpenter, B., Yao, Y., Kennedy, L., Gabry, J., Bürkner, P.-C., and Modrák, M. (2020). Bayesian workflow. *arXiv:2011.01808*.

- Gelman, A. and Yao, Y. (2020). Holes in bayesian statistics. *Journal of Physics G: Nuclear and Particle Physics*, 48(1):014002.
- Ghitza, Y. and Gelman, A. (2013). Deep interactions with MRP: Election turnout and voting patterns among small electoral subgroups. *American Journal of Political Science*, 57(3):762–776.
- Gneiting, T. and Raftery, A. E. (2007). Strictly proper scoring rules, prediction, and estimation. *Journal of the American statistical Association*, 102(477):359–378.
- Gneiting, T. and Ranjan, R. (2011). Comparing density forecasts using threshold-and quantile-weighted scoring rules. *Journal of Business & Economic Statistics*, 29(3):411–422.
- Grünwald, P. and Van Ommen, T. (2017). Inconsistency of Bayesian inference for misspecified linear models, and a proposal for repairing it. *Bayesian Analysis*, 12(4).
- He, K., Zhang, X., Ren, S., and Sun, J. (2016). Deep residual learning for image recognition. In *IEEE Conference on Computer Vision and Pattern Recognition*, pages 770–778.
- Hermans, J., Begy, V., and Louppe, G. (2020). Likelihood-free MCMC with amortized approximate ratio estimators. In *International Conference on Machine Learning*, pages 4239–4248.
- Hinton, G., Srivastava, N., and Swersky, K. (2012). Overview of mini-batch gradient descent. *Technical Report*.
- Hoffman, M. D. and Gelman, A. (2014). The No-U-Turn sampler: adaptively setting path lengths in Hamiltonian Monte Carlo. *Journal of Machine Learning Research*, 15(1):1593–1623.
- Huggins, J. H. and Miller, J. W. (2023). Reproducible model selection using bagged posteriors. *Bayesian Analysis*, 18(1):79.
- Jankowiak, M., Pleiss, G., and Gardner, J. (2020). Parametric Gaussian process regressors. In *International conference on machine learning*, pages 4702–4712. PMLR.
- Jiang, W. and Tanner, M. A. (2008). Gibbs posterior for variable selection in high-dimensional classification and data mining. *Annals of Statistics*.
- Jordan, M. I., Ghahramani, Z., Jaakkola, T. S., and Saul, L. K. (1999). An introduction to variational methods for graphical models. *Machine Learning*, 37:183–233.
- Kéry, M. and Schaub, M. (2011). *Bayesian population analysis using WinBUGS: a hierarchical perspective*. Academic press.
- Kingma, D. P. and Ba, J. (2015). Adam: A method for stochastic optimization.
- Knoblauch, J., Jewson, J., and Damoulas, T. (2022). An optimization-centric view on Bayes’ rule: Reviewing and generalizing variational inference. *Journal of Machine Learning Research*, 23(132):1–109.
- Kuśmierczyk, T., Sakaya, J., and Klami, A. (2019). Variational Bayesian decision-making for continuous utilities. *Advances in Neural Information Processing Systems*, 32.
- Lacoste-Julien, S., Huszár, F., and Ghahramani, Z. (2011). Approximate inference for the loss-calibrated Bayesian. In *International Conference on Artificial Intelligence and Statistics*, pages 416–424.
- Le, T. and Clarke, B. (2017). A bayes interpretation of stacking for m-complete and m-open settings. *Bayesian Analysis*.
- Louppe, G., Hermans, J., and Cranmer, K. (2019). Adversarial variational optimization of non-differentiable simulators. In *International Conference on Artificial Intelligence and Statistics*, pages 1438–1447.

- Magnusson, M., Torgander, J., Bürkner, P.-C., Zhang, L., Carpenter, B., and Vehtari, A. (2024). Posteriorodb: Testing, benchmarking and developing Bayesian inference algorithms. *arXiv:2407.04967*.
- Masegosa, A. (2020). Learning under model misspecification: Applications to variational and ensemble methods. *Advances in Neural Information Processing Systems*, 33:5479–5491.
- Matheson, J. E. and Winkler, R. L. (1976). Scoring rules for continuous probability distributions. *Management Science*, 22(10):1087–1096.
- Matsubara, T., Knoblauch, J., Briol, F.-X., and Oates, C. J. (2022). Robust generalised Bayesian inference for intractable likelihoods. *Journal of the Royal Statistical Society Series B*, 84(3):997–1022.
- McLatchie, Y., Cherief-Abdellatif, B.-E., Frazier, D. T., and Knoblauch, J. (2025). Predictively oriented posteriors. *arXiv preprint arXiv:2510.01915*.
- Morningstar, W. R., Alemi, A., and Dillon, J. V. (2022). PACm-Bayes: Narrowing the empirical risk gap in the misspecified Bayesian regime. In *International Conference on Artificial Intelligence and Statistics*, pages 8270–8298.
- Newey, W. K. and McFadden, D. (1994). Large sample estimation and hypothesis testing. *Handbook of Econometrics*, 4:2111–2245.
- Nogales, E. (2016). The development of Cryo-EM into a mainstream structural biology technique. *Nature Methods*, 13(1):24–27.
- Owen, A. B. (2013). *Monte Carlo theory, methods and examples*. <https://artowen.su.domains/mc/>.
- Papamakarios, G. and Murray, I. (2016). Fast ϵ -free inference of simulation models with Bayesian conditional density estimation. *Advances in Neural Information Processing Systems*, 29.
- Papamakarios, G., Nalisnick, E., Rezende, D. J., Mohamed, S., and Lakshminarayanan, B. (2021). Normalizing flows for probabilistic modeling and inference. *Journal of Machine Learning Research*, 22(57):1–64.
- Selten, R. (1998). Axiomatic characterization of the quadratic scoring rule. *Experimental Economics*, 1:43–61.
- Sheth, R. and Khardon, R. (2017). Excess risk bounds for the Bayes risk using variational inference in latent Gaussian models. *Advances in Neural Information Processing Systems*, 30.
- Sheth, R. and Khardon, R. (2020). Pseudo-Bayesian learning via direct loss minimization with applications to sparse Gaussian process models. In *Symposium on Advances in Approximate Bayesian Inference*, pages 1–18. PMLR.
- Singer, A. and Sigworth, F. J. (2020). Computational methods for single-particle electron cryomicroscopy. *Annual Review of Biomedical Data Science*, 3(1):163–190.
- Tejero-Cantero, A., Boelts, J., Deistler, M., Lueckmann, J.-M., Durkan, C., Gonçalves, P. J., Greenberg, D. S., and Macke, J. H. (2020). sbi: A toolkit for simulation-based inference. *Journal of Open Source Software*, 5(52):2505.
- Vandegar, M., Kagan, M., Wehenkel, A., and Louppe, G. (2021). Neural empirical Bayes: Source distribution estimation and its applications to simulation-based inference. In *International Conference on Artificial Intelligence and Statistics*, pages 2107–2115.
- Walker, S. G. (2013). Bayesian inference with misspecified models. *Journal of Statistical Planning and Inference*, 143(10):1621–1633.
- Wang, C. and Blei, D. M. (2018). A general method for robust Bayesian modeling. *Bayesian Analysis*.

- Wang, Y. and Blei, D. M. (2019). Variational Bayes under model misspecification. *Advances in Neural Information Processing Systems*, 32.
- Wang, Y., Miller, A. C., and Blei, D. M. (2019). Comment: Variational autoencoders as empirical Bayes. *Statistical Science*.
- Wenzel, F., Roth, K., Veeling, B. S., Światkowski, J., Tran, L., Mandt, S., Snoek, J., Salimans, T., Jenatton, R., and Nowozin, S. (2020). How good is the Bayes posterior in deep neural networks really? *International Conference on Machine Learning*.
- Whitesell, L. and Lindquist, S. L. (2005). HSP90 and the chaperoning of cancer. *Nature Reviews Cancer*, 5(10):761–772.
- Winkler, R. L. and Murphy, A. H. (1968). “good” probability assessors. *Journal of Applied Meteorology and Climatology*, 7(5):751–758.
- Yang, Z. and Zhu, T. (2018). Bayesian selection of misspecified models is overconfident and may cause spurious posterior probabilities for phylogenetic trees. *Proceedings of the National Academy of Sciences*, 115(8):1854–1859.
- Yao, Y., Régaldo-Saint Blancard, B., and Domke, J. (2024). Simulation-based stacking. In *International Conference on Artificial Intelligence and Statistics*, pages 4267–4275.
- Yao, Y., Vehtari, A., Simpson, D., and Gelman, A. (2018). Using stacking to average Bayesian predictive distributions. *Bayesian Analysis*, 13(3):917–1003.
- Zellner, A. (1988). Optimal information processing and Bayes’s theorem. *The American Statistician*, 42(4):278–280.
- Zhang, T. (2006). Information-theoretic upper and lower bounds for statistical estimation. *IEEE Transactions on Information Theory*, 52(4):1307–1321.

Appendices to “Predictive Variational Inference”

In the appendices, we finish proofs and more discussion of the theory claims we made in the paper. We also provide details of our numerical experiments.

A. Proofs

A.1. Proof of Proposition 1

We restate Proposition 1 formally and prove the properties.

Proposition 1 (formal). *Suppose the variational distribution $q_\phi(\theta)$ is parameterized by $\phi \in \Phi$, where Φ is compact. With any strictly proper score function S , an unknown true data generating process distribution $p_{\text{true}}(y)$, a likelihood model $p(y|\theta)$, and a size- n sample $y_1, y_2, \dots, y_n \sim p_{\text{true}}(\cdot)$, let ϕ_n be the solution of the PVI objective with a continuous prior regularization on ϕ*

$$\phi_n = \operatorname{argmax}_{\phi \in \Phi} \left(\sum_{i=1}^n S \left(\int p(\cdot|\theta) q_\phi(\theta) d\theta, y_i \right) - \lambda r^{\text{prior}}(\phi) \right). \quad (7)$$

The predictively optimal variational parameter ϕ_0 is defined as

$$\phi_0 := \operatorname{argmax}_{\phi \in \Phi} S \left(\int p(\cdot|\theta) q_\phi(\theta) d\theta, p_{\text{true}}(\cdot) \right).$$

Define $\ell(y, \phi) = S(\int p(\cdot|\theta) q_\phi(\theta) d\theta, y)$, then we have (1) consistency: if $\mathbb{E}_{y \sim p_{\text{true}}} [\sup_{\phi \in \Phi} |\ell(y, \phi)|] < \infty$, ϕ_0 is unique, and $\ell(y_i, \phi)$ is continuous at each $\phi \in \Phi$, then $\phi_n \xrightarrow{P} \phi_0$ as $n \rightarrow \infty$; (2) asymptotic normality: if additionally, $\phi_0 \in \text{interior}(\Phi)$, $\ell(y_i, \phi)$ is twice continuously differentiable, $\sqrt{n} \nabla_\phi \frac{1}{n} \sum_{i=1}^n \ell(y_i, \phi) \xrightarrow{d} \mathcal{N}(0, \Sigma)$, and $\sup_\phi \|\nabla_\phi^2 \frac{1}{n} \sum_{i=1}^n \ell(y_i, \phi) - H(\phi)\| \xrightarrow{P} 0$ for a continuous $H(\phi)$, and let $H = H(\phi_0)$ which is not singular, then $\sqrt{n}(\phi_n - \phi_0) \xrightarrow{d} \mathcal{N}(0, H^{-1}\Sigma H^{-1})$.

Proof. The proof is technically the same as the convergence and asymptotic normality of MLE, with additional consideration of the regularization. There exist other sets of assumptions that lead to the same results. To simplify the notations here, we define

$$\begin{aligned} T(\phi) &= S \left(\int p(\cdot|\theta) q_\phi(\theta) d\theta, p_{\text{true}}(\cdot) \right), \\ T'_n(\phi) &= \frac{1}{n} \sum_{i=1}^n \ell(y_i, \phi), \\ d(y) &= \sup_{\phi \in \Phi} |\ell(y, \phi)|. \end{aligned}$$

Then $\phi_0 = \operatorname{argmax}_{\phi \in \Phi} T(\phi)$ and define $\phi'_n = \operatorname{argmax}_{\phi \in \Phi} T'_n(\phi)$. Our assumption says that $\ell(y_i, \phi)$ is continuous at each ϕ and $|\ell(y, \phi)| \leq d(y)$ for $\mathbb{E}_{y \sim p_{\text{true}}} [d(y)] < \infty$. With dominated convergence theorem, $T(\phi) = \mathbb{E}_{y \sim p_{\text{true}}} [\ell(y, \phi)]$ is continuous on ϕ . Using uniform law of large numbers,

$$\sup_{\phi \in \Phi} |T'_n(\phi) - T(\phi)| \xrightarrow{P} 0. \quad (8)$$

This basically implies the convergence result when $\lambda = 0$. Next, we define

$$T_n(\phi) = \frac{1}{n} \sum_{i=1}^n \ell(y_i, \phi) - \frac{\lambda}{n} r^{\text{prior}}(\phi),$$

such that $\phi_n = \operatorname{argmax}_{\phi \in \Phi} T_n(\phi)$. As Φ is compact, there exists U such that $0 \leq r^{\text{prior}}(\phi) \leq U$. Hence $\sup_{\phi \in \Phi} |T_n(\phi) - T'_n(\phi)| \rightarrow 0$. Along with (8), we have that

$$\sup_{\phi \in \Phi} |T_n(\phi) - T(\phi)| \xrightarrow{P} 0.$$

With Theorem 2.1 in [Newey and McFadden \(1994\)](#), we have $\phi_n \xrightarrow{P} \phi_0$.

For asymptotic normality, note that $\nabla_{\phi} \lambda r^{\text{prior}}(\phi) = \mathcal{O}(1/n)$ and $\nabla_{\phi}^2 \lambda r^{\text{prior}}(\phi) \rightarrow 0$, so we further have $\sqrt{n} \nabla_{\phi} T_n(\phi) \xrightarrow{d} \mathcal{N}(0, \Sigma)$, and $\sup_{\phi} \|\nabla_{\phi}^2 T_n(\phi) - H(\phi)\| \xrightarrow{P} 0$. With Theorem 3.1 in [Newey and McFadden \(1994\)](#), we also have the asymptotic normality. \square

Note we have an assumption that ϕ_0 is unique. However, PVI is typically overparametrized: the PVI optimal solution may not be unique. Even in a normal model, $y \sim \text{normal}(\mu, \sigma)$, when both μ and σ are allowed to be non-degenerating random variables, it is equivalent to distribute uncertainty either on the variance of μ , or on the scale of σ^2 . We are not worried about overparameterization for three reasons. (1) In practice, we proposed to use regularization to break the ties, such that numerical optimization is often not an issue. (2) In our view, this overparameterization allows PVI to adjust for model misspecification to achieve better predictive performance. (3) Since we are using normalizing flows, even when the PVI solution is unique, the flow parameter will not be unique because a normalizing flow itself is typically not identifiable. Nevertheless, the overparameterization should not prevent PVI from being useful. We include the uniqueness assumption in Proposition 1 for theory interests. There is one special case when the uniqueness is typically satisfied—when the parametric model is ‘correct’ and the PVI optimum is a point delta function. Then our uniqueness assumption becomes the usual identifiable assumption of the original model, which is typically met. The main theoretical interest of Proposition 1 is to establish the consistency and convergence rate of PVI, such that it is ‘backward compatible’ with the regular Bayes when the model is correct.

A.2. Unbiased rejection sampling for the Logarithmic score gradient

We propose a rejection sampling typed gradient estimate for each $g_i^{\log}(\phi) = \frac{d}{d\phi} \log \int p(y_i|\theta) q_{\phi}(\theta) d\theta$ under log score. It is particularly simple when the pointwise likelihood $p(y_i|\theta)$ is bounded. That is, there exists a known scaler constant $C > 0$ such that $p(y_i|\theta) < C$ for all i and $\theta \in \Theta$. We will discuss this boundness condition later.

At each SGD iteration given a ϕ , we draw M i.i.d. copies $\theta_1, \dots, \theta_M$ from $q_{\phi}(\theta)$, and M i.i.d. copies t_1, \dots, t_M from Uniform(0,1) distribution. Pointwise, we compute $p(y_i|\theta_j)/C$, if $t_j < p(y_i|\theta_j)/C$ then we accept the draw θ_j . If at least one draw is accepted, we approximate the gradient $g_i^{\log}(\phi)$ by

$$g_i^{\text{RS}} := \frac{\sum_{j=1}^M \left(\mathbb{1}(t_j < p(y_i|\theta_j)/C) \frac{\partial}{\partial \phi} \log q_{\phi}(\theta_j) \right)}{\sum_{j=1}^M \mathbb{1}(t_j < p(y_i|\theta_j)/C)}. \quad (9)$$

If none of the draws are accepted, we resample $\theta_1, \dots, \theta_M$ and t_1, \dots, t_M until we have an estimator. Finally we compute $g^{\text{RS}} = \sum_{i=1}^n g_i^{\text{RS}}$.

Shifting from importance sampling to rejection sampling seems a small step change, but it ensures an unbiased gradient estimate even with one Monte Carlo draw, i.e.,

Proposition 4. For any sample size $M \geq 1$, $\mathbb{E}_{\theta, t}[g_i^{\text{RS}}] = g_i^{\log}(\phi)$.

Proof. Without the loss of generality, assume $C = 1$. We first show that each g_i^{RS} is an unbiased estimator for $g_i^{\log}(\phi)$. We consider a sub-sequence of the auxiliary samples $t_{n_1}, t_{n_2}, \dots, t_{n_k}$, where

$1 \leq n_1 < n_2 < \dots < n_k \leq M$ and $N = \{n_1, \dots, n_k\}$ is the set of indexes, and condition on the case where their draws are accepted but others are rejected. Denote the predictive distribution by $q_\phi^Y(y_i) = \int p(y_i|\theta)q_\phi(\theta)d\theta$. Then we have

$$\begin{aligned}
& \mathbb{E}[g_i^{\text{RS}} | \text{accept } t_{n_1}, \dots, t_{n_k}] \\
&= \frac{\mathbb{E}_{\text{accept } t_{n_1}, \dots, t_{n_k}} [g_i^{\text{RS}}]}{P(\text{accept } t_{n_1}, \dots, t_{n_k})} \\
&= \frac{\int \dots \int \prod_{m=1}^M q_\phi(\theta_m) \prod_{j=1}^k p(y_i|\theta_{n_j}) \prod_{j \notin N} (1 - p(y_i|\theta_j))^{\frac{1}{k}} \sum_{j=1}^k \frac{\partial}{\partial \phi} \log q_\phi(\theta_{n_j}) d\Theta}{\int \dots \int \prod_{m=1}^M q_\phi(\theta_m) \prod_{j=1}^k p(y_i|\theta_{n_j}) \prod_{j \notin N} (1 - p(y_i|\theta_j)) d\Theta} \\
&= \frac{\int \dots \int \prod_{j \notin N} q_\phi(\theta_j) (1 - p(y_i|\theta_j))^{\frac{1}{k}} \sum_{l=1}^k \int \dots \int p(y_i|\theta_{n_l}) \frac{\partial}{\partial \phi} q_\phi(\theta_{n_l}) \prod_{j=1}^{k, j \neq l} q_\phi(\theta_{n_j}) p(y_i|\theta_{n_j}) d\Theta_N d\Theta_{-N}}{\int \dots \int \prod_{j \notin N} q_\phi(\theta_j) (1 - p(y_i|\theta_j)) \int \dots \int \prod_{j=1}^k q_\phi(\theta_{n_j}) p(y_i|\theta_{n_j}) d\Theta_N d\Theta_{-N}} \\
&= \frac{\int \dots \int \prod_{j \notin N} q_\phi(\theta_j) (1 - p(y_i|\theta_j))^{\frac{1}{k}} \sum_{l=1}^k q_\phi^Y(y_i)^{k-1} \frac{\partial}{\partial \theta} q_\phi^Y(y_i) d\Theta_{-N}}{\int \dots \int \prod_{j \notin N} q_\phi(\theta_j) (1 - p(y_i|\theta_j)) q_\phi^Y(y_i)^k d\Theta_{-N}} \\
&= \frac{q_\phi^Y(y_i)^{k-1} \frac{\partial}{\partial \theta} q_\phi^Y(y_i)}{q_\phi^Y(y_i)^k} \\
&= g_i^{\log}(\phi).
\end{aligned}$$

Collecting all cases of acceptance, we directly have $\mathbb{E}[g_i^{\text{RS}}] = g_i^{\log}(\phi)$. \square

At a high level, the gradient estimator in the main text is only asymptotically unbiased, while unnormalized rejection sampling is unbiased with any sample size, hence more suitable for SGD.

Bounded likelihood. The assumption on the bounded likelihood can be achieved at two general settings, (1) the observations are discrete thereby $p_i(y_i|\theta) \leq 1$, and (2) the likelihood has a fixed non-zero variance. For example in a one-dimensional linear regression problem, the likelihood is $p(y|\beta, \sigma) = \text{normal}(y|\beta X, \sigma)$, if σ is fixed to be a small number, then $M = (\sqrt{2\pi}\sigma)^{-1}$.

A fixed σ is less evil than it seems. First, the model is over parametrized, the observational noise can either be learned from σ , or the variational variance of the constant feature. Second, PVI allows a more general inference paradigm, where ϕ contains both the variational parameters and those parameters that we would wish to learn by point estimate, which will then contain this σ . Indeed, the rejection sampling idea is still applicable when $M = M(\phi)$ depends on ϕ , and varies across SGD iterations.

In practice, however, we find that the benefits of having an unbiased estimator is not significant compared with the biased estimator in the main paper. This coincides with the findings of another unbiased estimator derived in Vandegar et al. (2021), which is also found not beneficial when the Monte Carlo sample size is large.

A.3. Convergence of the logarithmic score gradient

For the logarithmic score

$$\mathcal{L}^{\log}(\phi) = \sum_{i=1}^n \log \int_{\Theta} p(y_i|\theta)q_\phi(\theta)d\theta,$$

we have a gradient estimator

$$g_M^{\log}(\phi) = \sum_{i=1}^n \frac{\sum_{j=1}^M \frac{d}{d\phi} p(y_i | T_\phi(u_j))}{\sum_{j=1}^M p(y_i | T_\phi(u_j))}$$

after reparameterization of $\theta = T_\phi(u)$ and with M samples of u_1, \dots, u_M . We first show that it converges in probability.

Proposition 5. *As $M \rightarrow \infty$, $g_M^{\log}(\phi) \xrightarrow{P} \frac{d}{d\phi} \mathcal{L}^{\log}(\phi)$.*

Proof. Define $\theta_j = T_\phi(u_j)$, $A_M = \frac{1}{M} \sum_{j=1}^M \frac{d}{d\phi} p(y|\theta_j)$, $B_M = \frac{1}{M} \sum_{j=1}^M p(y|\theta_j)$. To prove the convergence, it is enough to show for any y ,

$$\frac{A_M}{B_M} \xrightarrow{P} \frac{d}{d\phi} \log \int_{\Theta} p(y|\theta) q_\phi(\theta) d\theta.$$

Note $A_M \xrightarrow{P} \int_{\Theta} \frac{d}{d\phi} p(y|\theta) q_\phi(\theta) d\theta$ and $B_M \xrightarrow{P} \int_{\Theta} p(y|\theta) q_\phi(\theta) d\theta$ under regularity conditions. By Slutsky's theorem, we have that $A_M/B_M \xrightarrow{P} \frac{d}{d\phi} \log \int_{\Theta} p(y|\theta) q_\phi(\theta) d\theta$. \square

Note the gradient estimator has the same form as a self-normalized importance sampling estimator, which converges almost surely. The bias of a self-normalized importance sampling estimator is also known to converge to zero approximately at the rate of $\mathcal{O}(M^{-1})$. See [Owen \(2013\)](#) for more details.

A.4. Convergence of the quardartic score gradient

For the quadratic score

$$\mathcal{L}^{\text{quad}}(\phi) = \sum_{i=1}^n 2 \int_{\Theta} f(\theta, y_i) q_\phi(\theta) d\theta - \sum_{j=1}^I \left(\int_{\Theta} f(\theta, j) q_\phi(\theta) d\theta \right)^2,$$

we have a gradient estimator

$$g_M^{\text{quad}}(\phi) = 2 \sum_{i=1}^n \frac{1}{M} \sum_{j=1}^M f(T_\phi(u_j), y_i) - \sum_{j=1}^I \left(\frac{1}{M} \sum_{k=1}^M f(T_\phi(u_k), j) \right) \left(\frac{1}{M} \sum_{k=1}^M \frac{df(T_\phi(u_k), j)}{d\phi} \right).$$

We have the same result of converging in probability.

Proposition 6. *As $M \rightarrow \infty$, $g_M^{\text{quad}}(\phi) \xrightarrow{P} \frac{d}{d\phi} \mathcal{L}^{\text{quad}}(\phi)$.*

Proof. Define $\theta_k = T_\phi(u_k)$, $A_{M,j} = \frac{1}{M} \sum_{k=1}^M \frac{d}{d\phi} f(\theta_k, j)$, $B_{M,j} = \frac{1}{M} \sum_{k=1}^M f(\theta_k, j)$. Note for any j , $A_{M,j} \xrightarrow{P} \frac{d}{d\phi} \int_{\Theta} f(\theta, j) q_\phi(\theta) d\theta$ and $B_{M,j} \xrightarrow{P} \int_{\Theta} f(\theta, j) q_\phi(\theta) d\theta$ under regularity conditions. Then, for a single y

$$\begin{aligned} & \frac{d}{d\phi} \left(2 \int_{\Theta} f(\theta, y) q_\phi(\theta) d\theta - \sum_{j=1}^I \left(\int_{\Theta} f(\theta, j) q_\phi(\theta) d\theta \right)^2 \right) \\ &= 2 \frac{d}{d\phi} \int_{\Theta} f(\theta, y) q_\phi(\theta) d\theta - 2 \sum_{j=1}^I \left(\int_{\Theta} f(\theta, j) q_\phi(\theta) d\theta \right) \frac{d}{d\phi} \left(\int_{\Theta} f(\theta, j) q_\phi(\theta) d\theta \right) \\ &\approx 2A_{M,y} - 2 \sum_{j=1}^I B_{M,j} A_{M,j}. \end{aligned}$$

By Slutsky's theorem, we have that $2A_{M,y} - 2\sum_{j=1}^I B_{M,j}A_{M,j}$ converges in probability for a single y . Thus the constructed gradient estimator also converges in probability. \square

A.5. Convergence of the interval score gradient

For the interval score objective

$$\mathcal{L}^{\text{IS}}(\phi) = -\sum_{i=1}^n (U_\alpha - L_\alpha) + \frac{2}{\alpha}(L_\alpha - y_i)\mathbb{I}(y_i < L_\alpha) + \frac{2}{\alpha}(y_i - U_\alpha)\mathbb{I}(y_i > U_\alpha), \quad (10)$$

the gradient estimator is

$$g_M^{\text{IS}}(\phi) = \sum_{i=1}^n \frac{\partial \hat{U}_\alpha}{\partial \phi} \left(\frac{2}{\alpha}\mathbb{I}(y_i > \hat{U}_\alpha) - 1 \right) - \frac{\partial \hat{L}_\alpha}{\partial \phi} \left(\frac{2}{\alpha}\mathbb{I}(y_i < \hat{L}_\alpha) - 1 \right), \quad (11)$$

where \hat{L}_α and \hat{U}_α are estimated from M samples $y_1^{\text{sim}}, y_2^{\text{sim}}, \dots, y_M^{\text{sim}}$ from $\int_{\Theta} p(y|\theta)q_\phi(\theta)d\theta$. We show that the gradient estimator is convergent.

Proposition 7. As $M \rightarrow \infty$, $g_M^{\text{IS}}(\phi) \xrightarrow{P} \frac{d}{d\phi}\mathcal{L}^{\text{IS}}(\phi)$.

Proof. There are two parts of the proof. First, $\frac{\partial \hat{L}_\alpha}{\partial \phi}$ and $\frac{\partial \hat{U}_\alpha}{\partial \phi}$ are obtained from autodiff. We show they are consistent. Consider the empirical quantile function $\hat{Q}_\gamma(\phi)$ for the M simulated samples. For any ϕ , by Glivenko-Cantelli theorem, $\hat{Q}_\gamma(\phi) \rightarrow Q_\gamma(\phi)$ almost surely. Under regularity conditions, with Attouch theorem, $\partial \hat{Q}_\gamma(\phi)$ converges graphically to $\partial Q_\gamma(\phi)$, which has a unique element $\frac{\partial Q_\gamma(\phi)}{\partial \phi}$. By applying with $\gamma = \alpha/2$ and $\gamma = 1 - \alpha/2$, we have both $\frac{\partial \hat{L}_\alpha}{\partial \phi}$ and $\frac{\partial \hat{U}_\alpha}{\partial \phi}$ are convergent.

Next, $\mathbb{I}(y_i > \hat{U}_\alpha)$ and $\mathbb{I}(y_i < \hat{L}_\alpha)$ converge in probability to the true indicator functions $\mathbb{I}(y_i > U_\alpha)$ and $\mathbb{I}(y_i < L_\alpha)$. So the combination of convergent gradient estimators converges in probability. This concludes the proof. \square

A.6. Unbiasedness of the CRPS gradient

For the CRPS objective

$$\mathcal{L}^{\text{CRPS}}(\phi) = -\sum_{i=1}^n \mathbb{E}_{y^{\text{sim}} \sim \int_{\Theta} p(y|\theta)q_\phi(\theta)d\theta} [|y^{\text{sim}} - y_i|] + \frac{1}{2} \mathbb{E}_{y_1^{\text{sim}}, y_2^{\text{sim}} \sim \int_{\Theta} p(y|\theta)q_\phi(\theta)d\theta} [|y_1^{\text{sim}} - y_2^{\text{sim}}|],$$

we have an unbiased estimator, assuming y^{sim} can be generated with reparameterization of $y^{\text{sim}} = \mathcal{T}_\phi(\epsilon)$, $\epsilon \sim q(\cdot)$. Such reparameterization is performed at both the variational distribution q_ϕ and the simulator $p(y|\theta)$. Then for an arbitrary y ,

$$\begin{aligned} \frac{d}{d\phi} \mathbb{E}_{y^{\text{sim}} \sim \int_{\Theta} p(y|\theta)q_\phi(\theta)d\theta} [|y^{\text{sim}} - y_i|] &= \mathbb{E}_{\epsilon \sim q(\cdot)} \left[\frac{d}{d\phi} |\mathcal{T}_\phi(\epsilon) - y| \right] \\ &\approx \frac{1}{2M} \sum_{m=1}^{2M} \text{sign}(\mathcal{T}_\phi(\epsilon_m) - y) \frac{d}{d\phi} \mathcal{T}_\phi(\epsilon_m) \\ &= \frac{1}{2M} \sum_{m=1}^{2M} \text{sign}(y_m^{\text{sim}} - y) \frac{d}{d\phi} y_m^{\text{sim}}. \end{aligned}$$

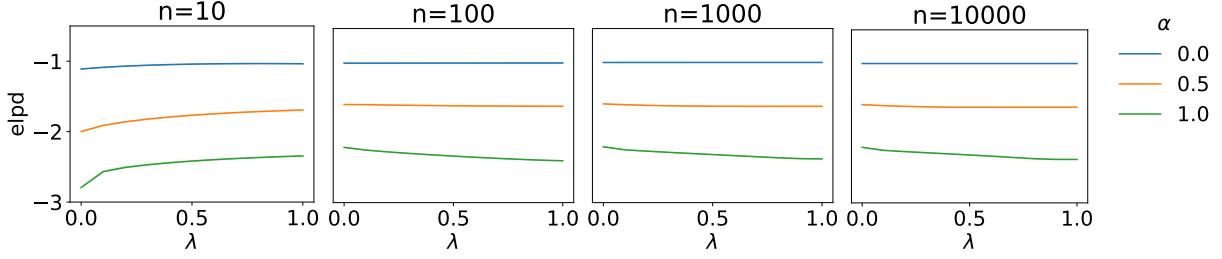


Figure 7: Test average elpd on a simple regression model, with different dataset sizes $n \in \{10, 100, 1000, 10000\}$ and specification scales α ($\alpha = 0$ for well-specified and $\alpha = 1$ for misspecified), interpolating between PVI ($\lambda = 0$) and VI ($\lambda = 1$). It is found that VI gives a better finite sample performance but PVI works better asymptotically.

Similarly, we have

$$\begin{aligned}
\frac{d}{d\phi} \mathbb{E}_{y_1^{\text{sim}}, y_2^{\text{sim}} \sim \int_{\Theta} p(y|\theta) q_{\phi}(\theta) d\theta} [|y_1^{\text{sim}} - y_2^{\text{sim}}|] &= \mathbb{E}_{\epsilon_a, \epsilon_b \sim q(\cdot)} \left[\frac{d}{d\phi} |\mathcal{T}_{\phi}(\epsilon_a) - \mathcal{T}_{\phi}(\epsilon_b)| \right] \\
&\approx \frac{1}{M} \sum_{m=1}^M \text{sign}(\mathcal{T}_{\phi}(\epsilon_m) - \mathcal{T}_{\phi}(\epsilon_{m+M})) \frac{d}{d\phi} (\mathcal{T}_{\phi}(\epsilon_m) - \mathcal{T}_{\phi}(\epsilon_{m+M})) \\
&= \frac{1}{M} \sum_{m=1}^M \text{sign}(y_m^{\text{sim}} - y_{m+M}^{\text{sim}}) \frac{d}{d\phi} (y_m^{\text{sim}} - y_{m+M}^{\text{sim}}).
\end{aligned}$$

Both Monte Carlo estimators are unbiased and we directly have an unbiased gradient estimator for CRPS:

$$g^{\text{CRPS}}(\phi) = -\frac{1}{2M} \sum_{i=1}^n \sum_{m=1}^{2M} (g_m \cdot \text{sign}(y_m^{\text{sim}} - y_i)) + \frac{1}{2M} \sum_{m=1}^M ((g_m - g_{m+M}) \cdot \text{sign}(y_m^{\text{sim}} + y_{m+M}^{\text{sim}})),$$

where $g_m = \frac{d}{d\phi} y_m^{\text{sim}}$.

B. Additional Results and Experiments

We explore further properties of PVI through three simulated regression models, an example in linear regression, and additional benchmarks.

B.1. Interpolation between VI and PVI

Posterior regularization allows us to interpolate between VI and PVI. We expect that VI has good finite sample performance by having the prior while PVI has better performance asymptotically when the model is misspecified. We consider the regression problem:

$$y_i = \mathbf{x}_i^T \boldsymbol{\beta} + \epsilon, \quad \epsilon \sim \text{Normal}(0, 1),$$

where $y_i \in \mathbb{R}$, $\mathbf{x}_i \in \mathbb{R}^d$, $\boldsymbol{\beta} \in \mathbb{R}^d$ for datapoint $i \in \{1, 2, \dots, n\}$. In the data generating process, we specify a parameter α to interpolate between a well-specified model ($\alpha = 0$) and a misspecified model ($\alpha = 1$). We generate a collection of parameters $\{\boldsymbol{\beta}_0, \boldsymbol{\beta}_1, \dots, \boldsymbol{\beta}_g\}$ and choose $\boldsymbol{\beta}$ from $\{(1 -$

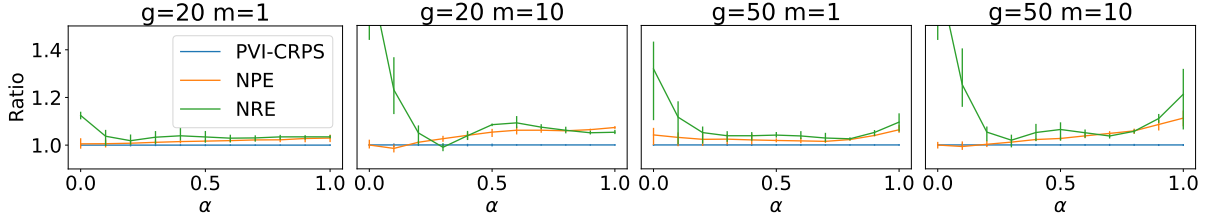


Figure 8: Ratios of test CRPS with respect to the test CRPS of PVI, with different parameters of the y^2 regression model (group number g , observation dimension m , misspecification scale α). We compare against NPE and NRE from SBI, showing that PVI is more favored especially when the model is misspecified ($\alpha \rightarrow 1$).

$\alpha)\beta_0 + \alpha\beta_j \mid j = 1, 2, \dots, g\}$ when generating each datapoint. The parameters are learned by a combined loss of VI and PVI. Namely, we maximize

$$\mathcal{L}_\lambda(\phi) = \lambda\mathcal{L}_{\text{VI}}(\phi) + (1 - \lambda)\mathcal{L}_{\text{PVI}}(\phi).$$

In Figure 7, the average elpd on the test set is plotted under different settings. We first focus on the dataset size. When $n = 10$, we note that the full PVI gives worse test predictive scores. This is reasonable as the learned parameters from PVI are entirely determined by limited number of samples, while VI is regularized by the prior. As the sample size n increases, PVI outperforms VI since it directly targets the prediction. We also note that on the correctly specified model $\alpha = 0$, PVI and VI are asymptotically equivalent. In practice, it is reasonable to have a combined objective of PVI and VI (which we call PVI with posterior regularization) for robust performances under different sample sizes and different models.

B.2. Likelihood-free regression

In regression problems, sometimes we are only able to access the summary statistics of groups of outcomes. This scenario is common in differential privacy and meta-analysis. We consider the same regression problem with more dimensions in the observation:

$$\mathbf{y}_i = \mathbf{X}_i\boldsymbol{\beta} + \boldsymbol{\epsilon}, \quad \boldsymbol{\epsilon} \sim \text{Normal}(\mathbf{0}, \mathbf{I}),$$

where $\mathbf{y}_i \in \mathbb{R}^m$, $\mathbf{X}_i \in \mathbb{R}^{m \times d}$, $\boldsymbol{\beta} \in \mathbb{R}^d$ for datapoint $i \in \{1, 2, \dots, n\}$. However, instead of the full vector \mathbf{y}_i , we only have access to $\hat{y}_i^2 := \sum_{j=1}^m y_{i,j}^2$. The likelihood of \hat{y}_i^2 follows non-central chi-squared distribution, whose probability density function involves an infinite summation. What's worse, the model may be mis-specified. In the data generating process, we specify a parameter α to interpolate between a well-specified model ($\alpha = 0$) and a mis-specified model ($\alpha = 1$). We generate a collection of parameters $\{\beta_0, \beta_1, \dots, \beta_g\}$ and choose $\boldsymbol{\beta}$ from $\{(1 - \alpha)\beta_0 + \alpha\beta_j \mid j = 1, 2, \dots, g\}$ for each datapoint. We compare PVI with CRPS against the standard implementations of neural posterior estimation (NPE) (Papamakarios and Murray, 2016) and neural ratio estimation (NRE) (Hermans et al., 2020) from SBI (Tejero-Cantero et al., 2020). Due to the Bayesian nature and the mis-specification of model their sequential counterparts perform worse.

First, we compare the performances of different methods with different interpolation parameters α . We find that PVI with CRPS has a robust performance under different levels of mis-specification. In addition, the performance gain is larger with more dimensions in observations (higher m). Note that the performance of NRE is good only with a modest level of misspecification. The good performance of NRE under modestly mis-specified case aligns with the findings in Cannon et al.

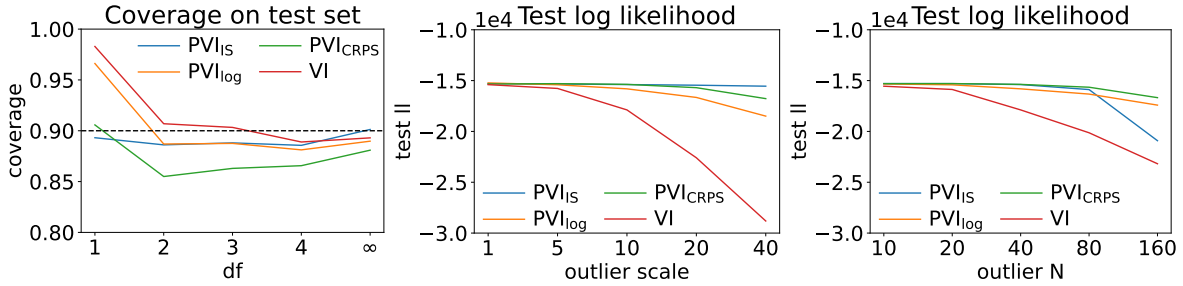


Figure 9: Comparing different scores with simulated regression model. Left: test coverage from PVI with different objectives with different Student- t noise models. Middle: test log likelihood from PVI with different objectives after mixing training data with 40 outliers of different scales. Right: test log likelihood from PVI with different objectives after mixing training data with different number of outliers of scale 10. In these experiments $n = 1000$. IS is trained with the significance level of $\alpha = 0.1$.

(2022), but we also show that eventually NRE can be as bad as NPE, as the problem of misspecification worsens.

B.3. Properties of different scoring rules

In theory, as $n \rightarrow \infty$, PVI will converge to the optimal parameter regardless of the scoring rule. In practice, different scoring rules have different finite sample behaviors and properties. We demonstrate the differences with a simple regression model. Suppose we have a true model $\mathbf{y}_i = \mathbf{x}_i^T \boldsymbol{\beta} + \epsilon$ where $\epsilon \sim t_{df}$. The model is mis-specified in two senses: there are multiple $\boldsymbol{\beta}$ s to generate data, and we use a normal model during inference. PVI is capable of handling these challenges. We find that the log score leads to the best test log likelihood. More interestingly, different scores lead to different test coverages. When training with IS on the confidence level of $\alpha = 0.1$, we consistently get correct test coverage that is not achieved by the other scoring rules. See the first panel of Fig. 9. This result demonstrates that PVI can potentially provide free conformal prediction with proper settings of the scoring rule. Next, we study the robustness of different scoring rules. During the data generating process, we insert noisy data of different scales into the training set. This mimics the real-world challenge of working with contaminated data. We first insert 4% of outliers into the training set and vary the scale of outliers. The test log likelihoods of different methods are in the second panel of Fig. 9. IS at the significance level of $\alpha = 0.1$ is the most robust to this type of contamination, followed by CRPS. This is because both IS and CRPS care about the calibration of the predictive distribution. Next, we keep the scale of outliers and vary the number of outliers. When there are 16% contaminated training data, the performance of IS with $\alpha = 0.1$ becomes much worse, as shown in Fig. 9. And CRPS is found to be the most robust to different sizes of contaminated data. This is because IS only works for a single significance level, while CRPS focuses on the global calibration at different locations.

B.4. The expressiveness of PVI

Another interesting view is that PVI expands the expressiveness of the underlying models by implicitly adding a layer of trainable parameters. We demonstrate this with an example in linear regression. Suppose our model is

$$y|x \sim \text{normal}(wx + b, \sigma),$$

and we have the variational distribution $q_\phi(\theta)$ where $\theta = [w, b, \sigma^2]$. If we assign a distribution over b and σ , the noise distribution is expanded to be a continuous mixture of normal distributions. PVI subsumes this case, which means if the posterior distribution is flexible enough, PVI can model arbitrary noise distributions for linear regression. This property can be generalized to other models with separable noise. Moreover, PVI also defines a distribution over w . In the general case, we have

$$\begin{aligned}\mathbb{E}_{\int p(y|x,\theta)q_\phi(\theta)d\theta}[y] &= \int \mathbb{E}_{p(y|x,\theta)}[y]q_\phi(\theta)d\theta \\ &= \mathbb{E}_{q_\phi(\theta)}[w]x + \mathbb{E}_{q_\phi(\theta)}[b], \\ \text{Var}_{\int p(y|x,\theta)q_\phi(\theta)d\theta}[y] &= \text{Var}_{q_\phi(\theta)}[\mathbb{E}_{p(y|x,\theta)}[y]] + \mathbb{E}_{q_\phi(\theta)}[\text{Var}_{p(y|x,\theta)}[y]] \\ &= \text{Var}_{q_\phi(\theta)}[wx + b] + \mathbb{E}_{q_\phi(\theta)}[\sigma^2] \\ &= \text{Var}_{q_\phi(\theta)}[w]x^2 + 2\text{Cov}_{q_\phi(\theta)}(w, b)x + \text{Var}_{q_\phi(\theta)}[b] + \mathbb{E}_{q_\phi(\sigma)}[\sigma^2].\end{aligned}$$

Although the resulting model still has a linear mean, the noise distribution can vary by location x , which is more expressive than models with stationary noise.

B.5. Benchmarking Stan models

We test PVI against vanilla VI on a collection of models from `posteriordb` (Magnusson et al., 2024) and evaluate their held-out data prediction performance. For each model, we use the same $M = 100$ Monte Carlo batch size. We perform a mild hyperparameter tuning in PVI (regularizer $r \in \{r^{\text{prior}}, r^{\text{post}}\}$, $\lambda \in \{0, 0.01, 0.1, 1\}$) by cross-validation. We consider two variational families, Gaussian with diagonal and dense covariance matrices, and compare each of the test scores on held-out data when possible. The results of both cases are shown in Table 2. We find that in general PVI always improves the prediction performance of the corresponding score on held-out data, a free model improvement. There are cases where PVI and VI are close (e.g., the election model and the radon model), which indicates that the model is nearly well-specified. Indeed, the election model here is saturated and passes the posterior predictive check as well.

C. Experiment settings

We detail the training settings of our major experiments. Since the experiments involve stochastic optimization and possibly mini-batching, we use the averaged score (or the empirical score) instead of the summations of scores as objectives in practice. The training involving the regression models and the `posteriordb` models are performed on a single Intel(R) Xeon(R) Gold 6126 CPU. The training involving the Cryo-EM model is performed on a single NVIDIA Tesla A100 GPU.

C.1. Election models

For the election models in Section 4.1, we train VI and PVI for 200,000 iterations using the learning rate of 10^{-5} , the RMSProp optimizer (Hinton et al., 2012) and Monte Carlo sample size $M = 100$. After 100,000 iterations the learning rate is reduced to 10^{-6} . The posterior is chosen to be full-rank Gaussian and no regularization is used for PVI.

C.2. Cryo-EM models

Each image of the generated protein is a gray-scale image with shape 128x128. To simulate real images, a defocus parameter of the microscope is sampled from [1000, 2000] and a Gaussian noise

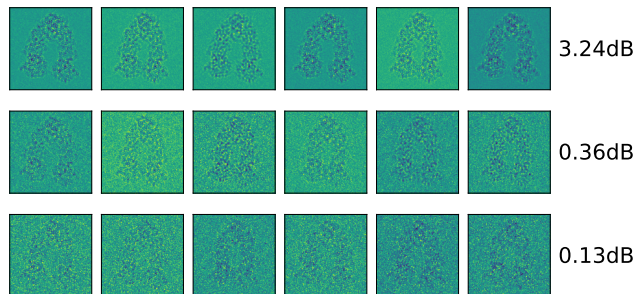


Figure 10: Examples of generated HSP90 protein images under different SNRs.

is added to the rendered image to reduce the SNR. See Figure 10 for generated noisy images under different noise scales. The noises in images makes the inference task very challenging.

Figure 1 in the main paper demonstrates the concentration of the posterior from the model $p^{\text{prior}}(\theta) \prod_{i=1}^n p(y_i|\theta)$. As we assume likelihood-free in this model, the Bayes posterior is approximated by learning a ResNet (He et al., 2016) based neural ratio estimation (Hermans et al., 2020) with a convolutional embedding network and sampling using 10 independent chains of the No-U-Turn sampler (NUTS) (Hoffman and Gelman, 2014).

In all of the CryoEM experiments with the CRPS, we use Monte Carlo sample size $M = 32$ and mini-batch size 32 for the training objective. The variational distribution is chosen to be one-dimensional neural spline (Durkan et al., 2019) with 32 knots. The optimizer is Adam (Kingma and Ba, 2015) and the learning rate is scheduled with a linear warm-up to 10^{-3} in the first 1,000 steps, and a cosine annealing reducing to 10^{-4} in the remaining 9,000 steps.

C.3. Posteriordb models

For each of the datasets, we split 60/20/20 as training, validation and test sets. VI and PVI are trained on the posteriordb models for 200,000 iterations using the RMSProp optimizer and Monte Carlo sample size $M = 100$. Each model has a different learning rate as in Table 3. After 100,000 iterations the learning rate is reduced to 0.1 of the starting learning rate.

C.4. Additional regression models

In Supplement B.1, we demonstrate the interpolation between VI and PVI. Each of the experiments is performed with a learning rate of 10^{-3} for 20,000 iterations using the RMSProp optimizer.

In Supplement B.2, we compare PVI with CRPS against various baselines on a likelihood-free regression model. The dimension of the parameter β is chosen to be $d = 5$ and the number of observations is $n = 1,000$. The distribution of the parameter is approximated by a neural spline flow (Durkan et al., 2019). PVI is trained with $M = 100$ Monte Carlo samples using the Adam optimizer (Kingma and Ba, 2015) and the learning rate is scheduled with a linear warm-up to 10^{-5} in the first 1,000 steps, and a cosine annealing reducing to 10^{-6} in the remaining 49,000 steps. To stabilize the training of the flow, the global norm of the gradient is clipped to be at most 10. For the baselines, we use 50,000 simulated samples to train NPE, and 10,000 simulated samples to train NRE. The numbers are chosen to match the training and inference time of PVI. In addition, we use NUTS to sample from the model implied by NRE.

D. Formulations of the posterior models

We include the mathematical formulas of the posterior models in this section. The prior, if not specified, is chosen to be $\text{normal}(0, 1)$ for each variable.

D.1. election

The election model uses data from seven CBS News polls conducted during the week before the 1988 presidential election of United States (Gelman, 2007). There are in total $n = 11566$ datapoints. For data i , the age group $a_i \in \{1, 2, 3, 4\}$, education level $e_i \in \{1, 2, 3, 4\}$, state $s_i \in \{1, \dots, 51\}$, region $r_i \in \{1, 2, 3, 4, 5\}$, indicator of black ethnicity $b_i \in \{0, 1\}$, gender $g_i \in \{0, 1\}$, the Republican share of the vote for president in the state in the previous election $p_i \in [0, 1]$, and voter outcome $y_i \in \{0, 1\}$ are collected. The likelihood model is

$$y_i \sim \text{Bernoulli}(\text{Logit}^{-1}(\beta_0 + \beta_1 b_i + \beta_2 g_i + \beta_3 b_i g_i + \beta_4 p_i + \beta_{5,a_i} + \beta_{6,e_i} + \beta_{7,a_i,e_i} + \beta_{8,s_i} + \beta_{9,r_i})).$$

For $\beta_0, \beta_1, \beta_2, \beta_3, \beta_4$, we assign the prior $\text{normal}(0, 100)$. For $\beta_{5,\cdot}$, we assign the prior $\text{normal}(0, \sigma_a)$ where $\sigma_a \sim \text{log_normal}(3, 1)$. Similarly, for $\beta_{6,\cdot}$, we assign the prior $\text{normal}(0, \sigma_e)$ where $\sigma_e \sim \text{log_normal}(3, 1)$. For $\beta_{7,\cdot}$, we assign the prior $\text{normal}(0, \sigma_{ac})$ where $\sigma_{ac} \sim \text{log_normal}(3, 1)$. For $\beta_{8,\cdot}$, we assign the prior $\text{normal}(0, \sigma_s)$ where $\sigma_s \sim \text{log_normal}(3, 1)$. For $\beta_{9,\cdot}$, we assign the prior $\text{normal}(0, \sigma_r)$ where $\sigma_r \sim \text{log_normal}(3, 1)$.

D.2. glmm

The dataset contains simulated population counts of peregrines in various sites and years in the French Jura over 9 years (Kéry and Schaub, 2011). there are in total $n = 2072$ observations. For observation i , the site $s_i \in \{1, \dots, 235\}$, the year $y_i \in \{1, \dots, 9\}$ and the observed count c_i are generated. The likelihood model is

$$c_i \sim \text{Poisson}(\exp(\mu + \alpha_{s_i} + \epsilon_{y_i})).$$

We assign $\text{normal}(0, 10)$ as the prior for μ , $\text{normal}(0, \sigma_s)$ as the prior for α_{\cdot} , $\text{normal}(0, \sigma_y)$ as the prior for ϵ_{\cdot} , $\text{log_normal}(1, 1)$ as the prior for σ_s , and $\text{log_normal}(0, 1)$ as the prior for σ_y .

D.3. earnings

The dataset studies the effects of heights and gender to the income in dollars (Gelman, 2007). There are in total of $n = 1192$ observations. Each observation i contains the height $h_i \in \mathbb{R}^+$, the gender $g_i \in \{0, 1\}$ and the income $e_i \in \mathbb{R}^+$. The model is

$$\log e_i \sim \text{normal}(\beta_0 + \beta_1 h_i + \beta_2 g_i + \beta_3 h_i g_i, \sigma).$$

During processing of the dataset the heights are centered, so we assign $\text{normal}(0, 1)$ to all coefficients and $\text{log_normal}(0, 1)$ to σ as priors.

D.4. kidscore

The dataset contains cognitive test scores of three and four-year-old children (Gelman, 2007). Data is collected from $n = 434$ kids. For kid i , the IQ $q_i \in \mathbb{R}^+$, mom's IQ $m_i \in \mathbb{R}^+$ and mom's completion of high school $h_i \in \{0, 1\}$ are collected. The likelihood model is

$$q_i \sim \text{normal}(\beta_0 + \beta_1 h_i + \beta_2 m_i + \beta_3 h_i m_i, \sigma).$$

Also, we centered the data so $\text{normal}(0, 1)$ is assigned as prior to all coefficients and $\text{normal}^+(0, 1)$ is assigned to σ as prior.

D.5. nes

The dataset contains the party identification information of individuals from the national election study of United States in the year of 2000 (Gelman, 2007). There are $n = 476$ datapoints. Each datapoint i includes the party identification $p_i \in \{1, \dots, 7\}$ (1 is strong Democrat and 7 is strong Republican), real political ideology $d_i \in \{1, \dots, 7\}$ (1 is strong liberal and 7 is strong conservative), race $r_i \in \{0, 0.5, 1\}$, education level $e_i \in \{1, 2, 3, 4\}$, gender $g_i \in \{0, 1\}$, income percentile $l_i \in \{1, 2, 3, 4, 5\}$, age group $a_i \in \{1, 2, 3, 4\}$. The likelihood model contains multiple terms

$$p_i \sim \text{normal}(\beta_0 + \beta_1 d_i + \beta_2 r_i + \beta_3 \mathbb{I}(a_i = 2) + \beta_4 \mathbb{I}(a_i = 3) + \beta_5 \mathbb{I}(a_i = 4) + \beta_6 e_i + \beta_7 g_i + \beta_8 l_i, \sigma).$$

Still, $\text{normal}(0, 1)$ is assigned as prior to all coefficients and $\text{normal}^+(0, 1)$ is assigned to σ as prior.

D.6. radon

The dataset contains data of radon levels in 386 different counties in the USA (Gelman, 2007). $n = 12573$ measurements are collected. In the i th measurement, the county id $c_i \in \{1, \dots, 386\}$, the floor measure $f_i \in \{0, \dots, 9\}$ and the log-radon measurement r_i are collected. We work with the model

$$r_i \sim \text{normal}(\alpha_{c_i} + \beta_{c_i} f_i, \sigma).$$

Each $\alpha.$ is assigned the prior $\text{normal}(\mu_\alpha, \sigma_\alpha)$ and each $\beta.$ is assigned the prior $\text{normal}(\mu_\beta, \sigma_\beta)$. Furthermore, μ_α and μ_β are both assigned the prior $\text{normal}(0, 10)$. $\sigma, \sigma_\alpha, \sigma_\beta$ are all assigned the prior $\log_normal(0, 1)$.

D.7. wells

The dataset studies factors affecting the decision of households in Bangladesh to switch wells (Gelman, 2007). There are in total $n = 3020$ datapoints. Each datapoint i includes the arsenic level $a_i \in \mathbb{R}^+$, the distance to the closest known safe well $d_i \in \mathbb{R}^+$, years of education of household head $e_i \in \mathbb{R}^+$ and decision of switching the well $s_i \in \{0, 1\}$. The regression model is

$$s_i \sim \text{Bernoulli}(\text{Logit}^{-1}(\beta_0 + \beta_1 a_i + \beta_2 d_i + \beta_3 e_i + \beta_4 a_i d_i + \beta_5 a_i e_i + \beta_6 d_i e_i)).$$

After centering the data, the coefficients are all assigned $\text{normal}(0, 1)$ as priors.

Model	Method	Diagonal covariance			
		Log (\uparrow)	Quad (\uparrow)	CRPS (\downarrow)	IS ($\times 10^3$) (\downarrow)
election	VI	-1494.44 (0.01)	0.21 (0.00)	-	-
	PVI-Log	-1490.89 (0.01)	0.21 (0.00)	-	-
	PVI-Quad	-1603.60 (1.96)	0.25 (0.00)	-	-
glmm	VI	-1159.49 (0.60)	-	-	-
	PVI-Log	-1150.21 (0.09)	-	-	-
earnings	VI	-298.12 (0.05)	-	111.51 (0.03)	229.89 (0.12)
	PVI-Log	-288.69 (0.01)	-	108.49 (0.00)	233.88 (0.08)
	PVI-CRPS	-291.54 (0.12)	-	109.55 (0.03)	232.72 (0.18)
	PVI-IS	-1046.23 (897.24)	-	125.89 (0.60)	228.13 (3.64)
kidscore	VI	-590.67 (0.08)	-	4481.15 (0.59)	3664.73 (1.36)
	PVI-Log	-369.91 (0.04)	-	872.82 (0.60)	778.14 (0.75)
	PVI-CRPS	-370.27 (0.05)	-	875.74 (0.56)	752.10 (1.33)
	PVI-IS	-374.63 (0.05)	-	925.96 (0.64)	717.11 (0.43)
nes	VI	-185.71 (0.01)	-	91.42 (0.01)	94.83 (0.03)
	PVI-Log	-185.60 (0.09)	-	91.02 (0.01)	96.90 (0.82)
	PVI-CRPS	-187.15 (0.76)	-	87.81 (0.09)	102.81 (1.05)
	PVI-IS	-226.56 (22.08)	-	110.31 (0.25)	65.37 (0.70)
radon	VI	-3412.90 (0.11)	-	1338.01 (0.09)	35635.36 (40.07)
	PVI-Log	-3372.10 (0.08)	-	1333.02 (0.03)	41141.75 (34.70)
	PVI-CRPS	-3482.39 (2.41)	-	1323.71 (0.30)	39140.21 (45.48)
	PVI-IS	-3444.50 (0.49)	-	1363.77 (0.09)	37070.83 (57.80)
wells	VI	-393.64 (0.04)	0.18 (0.00)	-	-
	PVI-Log	-392.14 (0.02)	0.18 (0.00)	-	-
	PVI-Quad	-415.39 (0.77)	0.27 (0.01)	-	-

Model	Method	Dense covariance			
		Log (\uparrow)	Quad (\uparrow)	CRPS (\downarrow)	IS ($\times 10^3$) (\downarrow)
election	VI	-1493.80 (0.16)	0.21 (0.00)	-	-
	PVI-Log	-1493.64 (0.09)	0.20 (0.00)	-	-
	PVI-Quad	-1603.64 (2.04)	0.25 (0.00)	-	-
glmm	VI	-1161.63 (0.81)	-	-	-
	PVI-Log	-1149.00 (0.58)	-	-	-
earnings	VI	-298.18 (0.07)	-	111.60 (0.04)	229.94 (0.09)
	PVI-Log	-283.42 (0.60)	-	109.08 (0.17)	232.43 (0.53)
	PVI-CRPS	-284.29 (0.29)	-	108.78 (0.07)	231.98 (0.61)
	PVI-IS	-310.03 (2.82)	-	121.44 (1.76)	229.32 (4.41)
kidscore	VI	-590.71 (0.07)	-	4480.55 (0.50)	3664.71 (1.11)
	PVI-Log	-371.06 (0.11)	-	871.84 (0.93)	771.42 (1.76)
	PVI-CRPS	-370.51 (0.16)	-	867.66 (1.01)	764.86 (1.79)
	PVI-IS	-382.05 (0.14)	-	1001.33 (1.05)	722.39 (0.30)
nes	VI	-185.71 (0.03)	-	91.49 (0.02)	94.79 (0.15)
	PVI-Log	-184.87 (0.02)	-	90.70 (0.08)	96.98 (0.16)
	PVI-CRPS	-187.91 (0.66)	-	89.75 (0.53)	96.21 (2.75)
	PVI-IS	-194.99 (0.16)	-	104.42 (0.26)	68.41 (0.31)
radon	VI	-3411.69 (0.09)	-	1337.71 (0.05)	36044.18 (30.63)
	PVI-Log	-3415.79 (0.21)	-	1344.73 (0.16)	37498.42 (111.74)
	PVI-CRPS	-3495.78 (18.63)	-	1330.10 (5.81)	39010.02 (124.78)
	PVI-IS	-3487.35 (1.21)	-	1384.58 (0.63)	37367.99 (32.33)
wells	VI	-393.68 (0.01)	0.18 (0.00)	-	-
	PVI-Log	-391.02 (0.02)	0.18 (0.00)	-	-
	PVI-Quad	-415.40 (0.77)	0.27 (0.01)	-	-

Table 2: Test predictive score (mean and std from 5 random seeds) on 7 models from posteriordb with VI or PVI. We show that PVI is better in general when the prediction is evaluated in the corresponding scoring rule.

Model	election	glmm	earnings	kidscore	nes	radon	wells
Likelihood	Bernoulli	Poisson	Normal	Normal	Normal	Normal	Bernoulli
n	11566	2072	1192	434	476	12573	3020
Initial learning rate	10^{-5}	10^{-5}	10^{-4}	10^{-4}	10^{-5}	10^{-5}	10^{-5}

Table 3: Specifications of the posteriordb models.